

Testing tree level TeV scale type-I and type-II seesaw scenarios in μ TRISTAN

Arindam Das,^{1,2,*} Jinmian Li,^{3,†} Sanjoy Mandal,^{4,‡} Takaaki Nomura,^{3,§} and Rao Zhang^{3,¶}

¹*Institute for the Advancement of Higher Education, Hokkaido University, Sapporo 060-0817, Japan*

²*Department of Physics, Hokkaido University, Sapporo 060-0810, Japan*

³*College of Physics, Sichuan University, Chengdu 610065, China*

⁴*Korea Institute for Advanced Study, Seoul 02455, Korea*

We investigate TeV scale type-I and type-II seesaw scenarios at the tree level at the μ^+e^- and $\mu^+\mu^+$ colliders in the μ TRISTAN experiment. In minimal type-I seesaw scenario we consider two generations of Standard Model (SM) singlet heavy Majorana type Right Handed Neutrinos (RHNs) which couples with SM gauge boson through light-heavy neutrino mixing. We consider a minimal scenario where one (other) generation of the RHN dominantly couples with electron (muon). Generating events for the signal and generic SM backgrounds for the final states $e^-\nu jj$ and $\mu^+\nu jj$ from μ^+e^- collision at $\sqrt{s} = 346$ GeV and 1 ab^{-1} luminosity, we estimate limits on the light-heavy neutrino mixing angles with respect to heavy neutrino mass for two generations of the heavy neutrinos. Comparing with the existing limits we find such limits could be two orders of magnitude stronger than electroweak precision data. Further, we study the effect of doubly charged scalar boson (H^{++}) from the type-II seesaw scenario in $\mu^+\mu^+$ collision at $\sqrt{s} = 2$ TeV. In this case we consider $\mu^+\mu^+ \rightarrow \ell_i^+\ell_j^+$ and $\mu^+\mu^+ \rightarrow H^{++}Z/\gamma$ processes followed by the same sign dilepton decay of H^{++} . We find that events involving e^+e^+ among these final states could provide significant difference between the normal and inverted orderings of the neutrino mass which could be probed in μ TRISTAN collider at 5σ significance in future.

I. INTRODUCTION

The origin of tiny neutrino mass and flavor mixing [1] is an unknown, long standing puzzle as Standard Model (SM) fails to explain it. It leads us to extend SM in a variety of ways to explain such interesting observation. Simply a dimension five operator [2] within SM opened the door to incorporate beyond the Standard Model (BSM) physics through particle extension of the SM. A fascinating approach to study such anomalies is to introduce SM-singlet heavy Majorana type Right Handed Neutrinos (RHNs) to generate tiny neutrino mass through suppression of a lepton number violating mass scale [3–8]- commonly recognized as type-I seesaw scenario. SM-singlet RHNs mix with the SM light neutrinos to interact with the SM gauge bosons and Higgs. However, RHNs are hitherto unidentified and considered that it could have mass from a light scale up to a very heavy scale depending on its role in a variety of theoretical aspects [9–18]. Recently LHC is also looking for prompt RHNs from same sign dilepton plus dijet and trilepton plus missing energy modes respectively to provide limits on the RHN mass and its mixing with light neutrinos [19–22].

Apart from the singlet fermion extension of the SM, there is another simple but interesting aspect where SM is extended by an $SU(2)$ triplet scalar with hypercharge $Y = +2$ arising as an UV-complete scenario of the dimension five operator. This scenario is called the type-II seesaw scenario [23–30]. Through the inclusion of the triplet scalar with small vacuum expectation value (VEV) v_Δ , Majorana type tiny neutrino mass in $\mathcal{O}(\text{eV})$ scale can be generated at the tree level followed by flavor mixing. Such a scenario could evolve large neutrino Yukawa coupling of $\mathcal{O}(1)$. Due to the gauge structure, the triplet (complex) scalar interacts with the SM gauge bosons, SM lepton and Higgs doublet developing a variety of decay modes of the triplet scalar [31, 32]. As a result such triplet scalars can be tested at high energy colliders following different decay modes of its doubly, singly charged and neutral scalar multiplets [33–39]. We point out that for $v_\Delta \leq 10^{-4}$, doubly charged Higgs dominantly decays into same sign dilepton mode whereas for $v_\Delta > 10^{-4}$, it decays into same sign W bosons. In the first case, doubly charged scalar mass below 1080 GeV [40] was not observed whereas in the second case the upper limit is around 350 GeV [41]. The singly charged and neutral multiplets from the type-II seesaw scenario have been tested at the LHC from gluon-fusion channels [42–47]. These processes are suppressed by an additional factor of $\mathcal{O}(v_\Delta^2)$ making them irrelevant for type-II seesaw scenario.

In this paper we study the tree level minimal type-I seesaw model at multi-TeV same sign muon collider or muon-positron collider [48–55] at μ TRISTAN experiment using ultra-cold anti-muon technology from J-PARC [56]. In this

* adas@particle.sci.hokudai.ac.jp

† jmli@scu.edu.cn

‡ smandal@kias.re.kr

§ nomura@scu.edu.cn

¶ zhangrao@stu.scu.edu.cn

experiment μ^+e^- collision could occur at $\sqrt{s} = 346$ GeV where μ^+ energy is $E_\mu = 1$ TeV and e^- energy is $E_e = 30$ GeV ($\sqrt{s} = 2\sqrt{E_\mu E_e}$) at 1 ab^{-1} luminosity. This could be upgraded to $\mu^+\mu^+$ collider at $\sqrt{s} = 2$ TeV or higher where muon energy is considered to be 1 TeV with 100 fb^{-1} luminosity or higher. Such a machine can potentially serve as a Higgs factory and participate in various phenomenological aspects [57–63] involving physics beyond the SM.

The unique initial state of the $\mu\text{TRISTAN}$ experiment allows us to study the tree level seesaw scenarios from interesting perspectives. In case of μ^+e^- collision we consider the heavy neutrino production from the type-I seesaw where only a t -channel W mediated scenario will appear provided the RHN mass (M_N) resides in the electroweak or TeV scale. Due to the light-heavy mixing, this process will be suppressed by modulus square of the respective mixing. We consider that there are two generations of RHNs which reside at the TeV scale and can be produced at the colliders. First generation of the RHNs (N_1) dominantly couple with the electron whereas the second generation (N_2) dominantly couples with muon. In this collider we can explore these two generations of RHNs and their corresponding mixing with electron and muon. The RHN produced in this scenario can dominantly decay into a muon in case of N_2 (electron in case of N_1) and W boson followed by the hadronic decay of its daughter W boson. Finally from the lepton and jets it could be possible to reconstruct the RHNs. Hence we can estimate the limits on mass and mixings of RHNs studying signal and corresponding SM backgrounds. For μ^+e^- collision we consider $45 \text{ GeV} \leq M_{N_{1,2}} \leq 340 \text{ GeV}$. In case of $\mu^+\mu^+$ collider we can study a unique behavior of the RHNs where a t -channel RHN mediated process could produce a pair of same sign W boson reflecting the Majorana nature of the heavy neutrino. However, this process is suppressed by the fourth power of the modulus of the mixing but it could be realized only in the collisions of same sign fermions.

In case of type-II seesaw scenario, $\mu^+\mu^+$ collision could play a crucial role to probe the effect of doubly charged scalar multiplet. In this case we consider two scenarios. In the first case we consider the doubly charged scalar mediated same-sign dilepton production scenario in the s -channel process accompanied by the t -channel same sign dilepton production mode mediated by SM neutral bosons. Here we prefer to consider non-muonic final states to reduce SM backgrounds. Followed by this scenario, we study the production of doubly charged scalar in association with Z boson or photon in the s -channel and t -channel. If Z boson is produced, then it is considered to decay into dominant mode of jets resulting a final state of same sign dilepton and two jets where same sign dileptons are produced from the doubly charged component of the triplet scalar. In case when doubly charged scalar is produced with a photon, the final state consists of a same sign dilepton from doubly charged scalar plus a photon. These processes are influenced by the Yukawa interaction between the left handed lepton doublet and scalar triplet following $SU(2)_L \otimes U(1)_Y$ gauge theory where we introduce recent neutrino oscillation data following two neutrino mass hierarchies, for example, normal ordering (NO) and inverted ordering (IO). In addition to that if we consider the same sign dilepton production process from doubly charged scalar and SM gauge bosons then we can compare left-right asymmetry (\mathcal{A}_{LR}) for the SM and doubly charged scalar induced processes. Here we consider one benchmark value for the triplet scalar mass as 1.03 TeV following the recent ATLAS study [40] at 140 fb^{-1} ruling out the possibility of a doubly charged scalar below 1 TeV.

The paper is arranged in the following way. In Sec. II we discuss the seesaw models at the tree level which could be tested at $\mu\text{TRISTAN}$ experiment. We give detailed analysis on the BSM searches in Sec. III followed by discussions on different limits on the model parameters, dependence on the neutrino oscillation. Finally we conclude our article in Sec. IV.

II. TESTABLE SEESAW MODELS AT THE TREE LEVEL

Among many proposals of neutrino mass generation mechanism, we discuss the tree level processes to generate neutrino mass which could reproduce the neutrino oscillation data and flavor mixing. These simple but interesting models are commonly known as type-I and type-II seesaw scenarios where SM-singlet heavy RHNs and $SU(2)_L$ triplet scalar with $Y = 2$ are introduced respectively. We discuss these models in following way:

Type-I seesaw

SM-singlet RHNs (N_R^β) are introduced to extend the SM which couples with SM lepton doublet (ℓ^α) and Higgs doublet (Φ). Hence we write down the relevant part of the Lagrangian as

$$\mathcal{L}_{\text{int}} \supset -y_D^{\alpha\beta} \bar{\ell}_L^\alpha \Phi N_R^\beta - \frac{1}{2} M_N^{\alpha\beta} \overline{N_R^{\alpha C}} N_R^\beta + H.c.. \quad (1)$$

where α and β stand for the generation indices. The second term in Eq. 1 is the lepton number violating Majorana mass term for the RHNs. After the electroweak symmetry is broken by the generation of VEV of the SM Higgs v_Φ , one

obtain the Dirac mass term of the neutrinos as $M_D = \frac{y_D v_\Phi}{\sqrt{2}}$. Hence we can write neutrino mass matrix incorporating the Dirac and Majorana masses in the following as

$$M_\nu = \begin{pmatrix} 0 & M_D \\ M_D^T & M_N \end{pmatrix}. \quad (2)$$

Now diagonalizing Eq. 2, the seesaw formula for the light Majorana neutrinos mass can be obtained as

$$m_\nu \simeq -M_D M_N^{-1} M_D^T. \quad (3)$$

To obtain a light neutrino mass of $\mathcal{O}(0.1)$ eV from a heavy RHN of mass M_N around $\mathcal{O}(100)$ GeV, the Dirac Yukawa coupling y_D could be $\mathcal{O}(10^{-6})$, however, the Y_D could reach at $\mathcal{O}(1)$ if general parametrization for the seesaw scenario is considered [64]. This scenario is considered in our article. We assume, $M_D M_N^{-1} \ll 1$ so that the light neutrino flavor eigenstates (ν) can be written in terms of the mass eigenstates of light neutrino (ν_m) and heavy neutrino (N_m) as $\nu \simeq \mathcal{N} \nu_m + V N_m$ where $V = M_D M_N^{-1}$ and $\mathcal{N} = (1 - \frac{1}{2}\epsilon) U_{\text{PMNS}}$ with $\epsilon = V^* V^T$ and U_{PMNS} is the usual neutrino mixing matrix applied to diagonalize m_ν in the following way

$$U_{\text{PMNS}}^T m_\nu U_{\text{PMNS}} = \text{diag}(m_1, m_2, m_3). \quad (4)$$

In presence of the parameter ϵ , mixing matrix \mathcal{N} is non-unitary [65–67]. Now we replace neutrino flavor eigenstates in charged current (CC) and neutral current (NC) interactions of the SM and obtain

$$\mathcal{L}_{\text{CC}} = -\frac{g}{\sqrt{2}} W_\mu \bar{e} \gamma^\mu P_L (\mathcal{N} \nu_m + V N_m) + \text{h.c.}, \quad (5)$$

where e denotes the three generations of the charged leptons in the vector form and

$$\mathcal{L}_{\text{NC}} = -\frac{g}{2c_w} Z_\mu [\bar{\nu}_m \gamma^\mu P_L (\mathcal{N}^\dagger \mathcal{N}) \nu_m + \overline{N_m} \gamma^\mu P_L (V^\dagger V) N_m + \{\bar{\nu}_m \gamma^\mu P_L (\mathcal{N}^\dagger V) N_m + \text{h.c.}\}], \quad (6)$$

where $c_w = \cos \theta_w$ is the weak mixing angle and projection operators are denoted as $P_{\text{L(R)}} = \frac{1}{2}(1 \mp \gamma_5)$. Because of non-unitarity \mathcal{N} , the flavor-changing neutral current could occur through the first term of Eq. (6) involving $\mathcal{N}^\dagger \mathcal{N}$ which is not equal to unity. In our scenario RHN mass is a free parameter. If RHN mass lies between 10 GeV $\leq M_N < M_W$, RHN undergoes three-body decay. The partial decay widths of N_i can be approximately given as

$$\Gamma(N_i \rightarrow \ell_\alpha^- \ell_\beta^+ \nu_{\ell_\beta}) = \Gamma(N_i \rightarrow \ell_\alpha^+ \ell_\beta^- \bar{\nu}_{\ell_\beta}) \simeq |V_{\alpha i}|^2 \frac{G_F^2}{192\pi^3} M_{N_i}^5 \quad (\alpha \neq \beta), \quad (7)$$

$$\begin{aligned} \Gamma(N_i \rightarrow \ell_\beta^- \ell_\beta^+ \nu_{\ell_\alpha}) &= \Gamma(N_i \rightarrow \ell_\beta^+ \ell_\beta^- \bar{\nu}_{\ell_\alpha}) \\ &\simeq |V_{\alpha i}|^2 \frac{G_F^2}{192\pi^3} M_{N_i}^5 \left(\frac{1}{4} \cos^2 2\theta_W + \sin^4 \theta_W \right) \quad (\alpha \neq \beta), \end{aligned} \quad (8)$$

$$\begin{aligned} \Gamma(N_i \rightarrow \ell_\alpha^- \ell_\alpha^+ \nu_{\ell_\alpha}) &= \Gamma(N_i \rightarrow \ell_\alpha^+ \ell_\alpha^- \bar{\nu}_{\ell_\alpha}) \\ &\simeq |V_{\alpha i}|^2 \frac{G_F^2}{192\pi^3} M_{N_i}^5 \left(\frac{1}{4} \cos^2 2\theta_W + \cos 2\theta_W + \sin^4 \theta_W \right), \end{aligned} \quad (9)$$

$$\Gamma(N_i \rightarrow \nu_\beta \bar{\nu}_\beta \nu_{\ell_\alpha}) = \Gamma(N_i \rightarrow \nu_\beta \bar{\nu}_\beta \bar{\nu}_{\ell_\alpha}) \simeq |V_{\alpha i}|^2 \frac{1}{4} \frac{G_F^2}{192\pi^3} M_{N_i}^5, \quad (10)$$

$$\Gamma(N_i \rightarrow \ell_\alpha^- q_a \bar{q}_b) = \Gamma(N_i \rightarrow \ell_\alpha^+ \bar{q}_a q_b) \simeq N_c |V_{\alpha i}|^2 |V_{\text{CKM}}^{ab}|^2 \frac{G_F^2}{192\pi^3} M_{N_i}^5, \quad (11)$$

$$\Gamma(N_i \rightarrow q_a \bar{q}_a \nu_{\ell_\alpha}) = \Gamma(N_i \rightarrow q_a \bar{q}_a \bar{\nu}_{\ell_\alpha}) \simeq N_c |V_{\alpha i}|^2 \frac{G_F^2}{192\pi^3} M_{N_i}^5 2 (|g_V^q|^2 + |g_A^q|^2), \quad (12)$$

where

$$\begin{aligned} g_V^u &= \frac{1}{2} - \frac{4}{3} \sin^2 \theta_W, \quad g_A^u = -\frac{1}{2}, \\ g_V^d &= -\frac{1}{2} + \frac{2}{3} \sin^2 \theta_W, \quad g_A^d = \frac{1}{2}, \end{aligned} \quad (13)$$

respectively which come from the interaction between Z boson and the quarks. $N_c = 3$ is the color factor for the quarks. If the RHNs are heavier than the SM gauge and scalar bosons then dominant two-body decay modes are $N \rightarrow \ell W$, $\nu_\ell Z$, $\nu_\ell h$, respectively and the corresponding partial decay widths can be given by

$$\begin{aligned} \Gamma(N_i \rightarrow \ell_\alpha W) &= \frac{g^2 |V_{i\alpha}|^2 (M_N^2 - M_W^2)^2 (M_N^2 + 2M_W^2)}{64\pi M_N^3 M_W^2}, \\ \Gamma(N_i \rightarrow \nu_\alpha Z) &= \frac{g^2 |V_{i\alpha}|^2 (M_N^2 - M_Z^2)^2 (M_N^2 + 2M_Z^2)}{128\pi c_w^2 M_N^3 M_Z^2}, \\ \Gamma(N_i \rightarrow \nu_\alpha h) &= \frac{|V_{i\alpha}|^2 (M_N^2 - M_h^2)^2}{32\pi M_N} \left(\frac{1}{v} \right)^2, \end{aligned} \quad (14)$$

respectively. The partial decay width of the heavy RHN into W^\pm being twice as large as into a neutral one due to the two degrees of freedom of W^\pm . In Fig. 1, we show the branching ratios of heavy neutrinos N_i to various final states

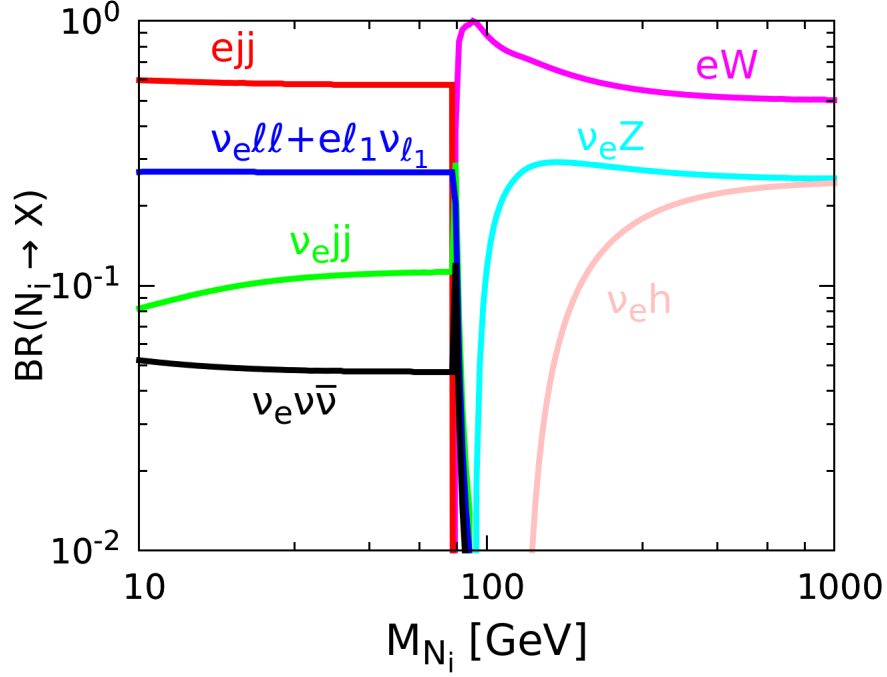


Figure 1. Branching ratios of N_i to different final states under the assumption $V_{eN_i} = 1, V_{\mu N_i} = 0$ and $V_{\tau N_i} = 0$. We show the branching ratios to three body leptonic channels $e\ell_1\nu_{\ell_1} + \nu_{e\ell\ell}, \nu_e\nu\bar{\nu}$ and semi-leptonic channels such as ejj and $\nu_e jj$, where $\ell = e, \mu, \tau, \ell_1 = \mu, \tau$. For relatively large M_{N_i} the two body decay channels such as $eW, \nu_e Z$ and $\nu_e h$ dominates. Similar behavior will be observed with the choice $V_{eN_i} = 0, V_{\mu N_i} = 1$ and $V_{\tau N_i} = 0$.

for $10 \text{ GeV} \leq M_N \leq 1000 \text{ GeV}$ assuming that $V_{eN_i} = 1, V_{\mu N_i} = 0$ and $V_{\tau N_i} = 0$. We point out that similar behavior will be observed with the choice $V_{eN_i} = 0, V_{\mu N_i} = 1$ and $V_{\tau N_i} = 0$. This is minimal scenario in case of type-I seesaw. For RHNS lighter than W boson ($M_N < M_W$) the dominant modes involve three body leptonic or semi-leptonic final states, whereas for RHNS heavier than W boson ($M_N > M_W$), two body decay modes dominate. Note that for very heavy RHNS where $M_N \geq \mathcal{O}(1) \text{ TeV}$ with non-zero light-heavy mixing, the branching ratios can be obtained as

$$\text{BR}(N_i \rightarrow \ell W) : \text{BR}(N_i \rightarrow \nu_\ell Z) : \text{BR}(N_i \rightarrow \nu_\ell h) = 2 : 1 : 1. \quad (15)$$

Note that for sufficiently small mixing and relatively small M_N , heavy RHNS could be long-lived candidates which that can travel a long distances before their decay into different daughter particles. This scenario gives rise to displaced vertex scenarios. We consider M_N and $|V_{\ell N_i}|^2$ as free parameters and $V_{\ell N_i}$ is always large enough so that RHNS suffer prompt decay.

Type-II seesaw scenario

In case of type-II seesaw scenario SM is extended by an $SU(2)_L$ triplet scalar $\Delta = (\Delta^{++}, \Delta^+, \Delta^0)^T$. The triplet scalar is described in the matrix form with the help of Pauli spin matrices as

$$\Delta = \begin{pmatrix} \Delta^+/\sqrt{2} & \Delta^{++} \\ \Delta^0 & -\Delta^+/\sqrt{2} \end{pmatrix}, \quad (16)$$

and due to its $SU(2)_L$ charge, it interacts with the SM gauge bosons. In addition to that it participates in a Yukawa coupling with SM lepton doublets. The corresponding Lagrangian with the scalar kinetic term can be written as

$$\mathcal{L}_{\text{type II}} = [iY_{\Delta\alpha\beta}L_\alpha^T C^{-1}\tau_2\Delta L_\beta + \text{h.c.}] + (D_\mu\Phi)^\dagger(D^\mu\Phi) + (D_\mu\Delta)^\dagger(D^\mu\Delta) - V(\Phi, \Delta), \quad (17)$$

where $Y_{\Delta}^{\alpha\beta}$ is the Yukawa coupling and it is a symmetric complex matrix. Here L_{α} represents SM lepton doublets, C stands for the charge conjugation operator, D_{μ} shows covariant derivative of the related scalar field and $V(\Phi, \Delta)$ is the scalar potential which could be expressed as

$$V(\Phi, \Delta) = -m_{\Phi}^2 \Phi^{\dagger} \Phi + \frac{\lambda}{4} (\Phi^{\dagger} \Phi)^2 + \tilde{M}_{\Delta}^2 \text{Tr} [\Delta^{\dagger} \Delta] + \lambda_2 [\text{Tr} \Delta^{\dagger} \Delta]^2 + \lambda_3 \text{Tr} [\Delta^{\dagger} \Delta]^2 + [\mu \Phi^T i \sigma_2 \Delta^{\dagger} \Phi + \text{h.c.}] + \lambda_1 (\Phi^{\dagger} \Phi) \text{Tr} [\Delta^{\dagger} \Delta] + \lambda_4 \Phi^{\dagger} \Delta \Delta^{\dagger} \Phi. \quad (18)$$

In this case Higgs triplet UV-completion of the Weinberg operator could be characterized by the induction of a tiny VEV of Δ . Minimizing the potential we find the mass-squared terms of the scalar fields as

$$\tilde{M}_{\Delta}^2 = M_{\Delta}^2 - \frac{1}{2} [2v_{\Delta}^2 (\lambda_2 + \lambda_3) + v_{\Phi}^2 (\lambda_1 + \lambda_4)], \quad \text{where } M_{\Delta}^2 \equiv \frac{v_{\Phi}^2 \mu}{\sqrt{2} v_{\Delta}}. \quad (19)$$

$$m_{\Phi}^2 = \frac{1}{2} \left[\frac{v_{\Phi}^2 \lambda}{2} + v_{\Delta}^2 (\lambda_1 + \lambda_4) - 2\sqrt{2} \mu v_{\Delta} \right]. \quad (20)$$

Solving Eq. (19) under the limit $M_{\Delta} \gg v_{\Phi}$ and satisfying all existing experimental limits we get

$$v_{\Delta} \approx \frac{\mu v_{\Phi}^2}{\sqrt{2} \tilde{M}_{\Delta}^2}, \quad (21)$$

keeping terms in first order of v_{Φ}/M_{Δ} . Hence using Eq. (17) and inserting the VEV of the triplet scalar, the neutrino mass from type-II seesaw can be estimated as

$$m_{\nu} = \sqrt{2} Y_{\Delta} v_{\Delta} = Y_{\Delta} \frac{\mu v_{\Phi}^2}{\tilde{M}_{\Delta}^2}. \quad (22)$$

Using neutrino oscillation data and $U_{\text{PMNS}}^T m_{\nu} U_{\text{PMNS}} = \text{diag}(m_1, m_2, m_3)$ to diagonalize the neutrino mass matrix we express

$$Y_{\Delta} = \frac{1}{2\sqrt{v_{\Delta}}} U_{\text{PMNS}} m_{\nu}^{\text{diag}} U_{\text{PMNS}}^T, \quad (23)$$

where $m_{\nu}^{\text{diag}} = \text{diag}(m_1, m_2, m_3)$, neutrino mass eigenvalues carry the information of neutrino oscillation for normal and inverted neutrino mass orderings along with U_{PMNS} which is the PMNS matrix. From Eq. (22) we find that neutrino mass is directly proportional to the triplet VEV. Therefore tiny neutrino mass can be ensured by small triplet VEV which could be satisfied either by a small trilinear term μ or being suppressed by a large \tilde{M}_{Δ} .

After spontaneous symmetry breaking we write the doublet and triplet fields as

$$\Delta = \frac{1}{\sqrt{2}} \begin{pmatrix} \Delta^+ & \sqrt{2} \Delta^{++} \\ v_{\Delta} + h_{\Delta} + i\eta_{\Delta} & -\Delta^+ \end{pmatrix}, \quad \Phi = \frac{1}{\sqrt{2}} \begin{pmatrix} \sqrt{2} \Phi^+ \\ v + h_{\Phi} + i\eta_{\Phi} \end{pmatrix}, \quad (24)$$

expanding the neutral multiplet around the VEV. In this model framework scalar sector contains ten degrees of freedom. After the electroweak symmetry breaking seven out of them have definite mass being evolved as physical fields. These scalar fields can be written as $H^{\pm\pm}$, H^{\pm} for the charged multiplets; h , H^0 and A^0 as neutral scalar fields respectively. Here $H^{\pm\pm}$ is simply $\Delta^{\pm\pm}$ as presented in the triplet scalar field Δ and the physical mass of H^{++} can be written as

$$m_{H^{++}}^2 = M_{\Delta}^2 - v_{\Delta}^2 \lambda_3 - \frac{\lambda_4}{2} v_{\Phi}^2. \quad (25)$$

The singly charged and neutral scalar mass eigenstates can be obtained by using 2×2 orthogonal rotation matrix as

$$\begin{pmatrix} \Phi^{\pm} \\ \Delta^{\pm} \end{pmatrix} = R(\beta_{\pm}) \begin{pmatrix} H^{\pm} \\ G^{\pm} \end{pmatrix}, \quad \begin{pmatrix} h_{\Phi} \\ h_{\Delta} \end{pmatrix} = R(\alpha) \begin{pmatrix} h \\ H^0 \end{pmatrix}, \\ \begin{pmatrix} \eta_{\Phi} \\ \eta_{\Delta} \end{pmatrix} = R(\beta_0) \begin{pmatrix} A^0 \\ G^0 \end{pmatrix}, \quad R(\theta) = \begin{pmatrix} \cos \theta & -\sin \theta \\ \sin \theta & \cos \theta \end{pmatrix},$$

where $\theta = \{\beta^{\pm}, \beta_0 \text{ and } \alpha\}$ are angle of rotation and $\tan \beta^{\pm} = \frac{\sqrt{2} v_{\Delta}}{v_{\Phi}}$, $\tan \beta_0 = \frac{2v_{\Delta}}{v_{\Phi}}$ and $\tan(2\alpha) = \frac{2B}{A-C}$ taking,

$$A = \frac{\lambda}{2} v_{\Phi}^2, \quad B = v_{\Phi} (-\sqrt{2} \mu + (\lambda_1 + \lambda_4) v_{\Delta}), \quad C = M_{\Delta}^2 + 2(\lambda_2 + \lambda_3) v_{\Delta}^2. \quad (26)$$

The charged scalar fields Φ^\pm from Φ and Δ^\pm from Δ are mixed to produce a physical H^\pm where an unphysical G^\pm is also identified as a Goldstone mode. Hence the physical mass of H^\pm can be written as

$$m_{H^\pm}^2 = \left(M_\Delta^2 - \frac{\lambda_4}{4} v_\Phi^2 \right) \left(1 + \frac{2v_\Delta^2}{v_\Phi^2} \right). \quad (27)$$

In the same line we find that CP-odd scalar A^0 and neutral Goldstone boson G^0 evolve from the mixture of η_Δ and η_Φ and hence G^0 becomes the longitudinal mode of Z boson. Now we find that the mass of the CP-odd scalar field A^0 can be written as

$$m_{A^0}^2 = M_\Delta^2 \left(1 + \frac{4v_\Delta^2}{v_\Phi^2} \right). \quad (28)$$

Finally, the CP-even scalar fields h_Δ from the neutral multiplet of Δ and h_Φ from Φ will mix and hence the SM Higgs (h) and a BSM neutral heavy Higgs (H^0) will evolve with physical masses as

$$m_h^2 = \frac{1}{2} [A + C - \sqrt{(A - C)^2 + 4B^2}], \quad (29)$$

$$m_{H^0}^2 = \frac{1}{2} [A + C + \sqrt{(A - C)^2 + 4B^2}] \quad (30)$$

respectively. The triplet VEV v_Δ could be constrained from the ρ parameter leading to upper bound of the triplet VEV as $\mathcal{O}(1 \text{ GeV})$ [1]. Hence using the fact $v_\Delta \ll v_\Phi$, the masses of physical Higgs bosons can be approximated as

$$m_{H^{\pm\pm}}^2 \simeq M_\Delta^2 - \frac{\lambda_4}{2} v_\Phi^2, \quad m_{H^\pm}^2 \simeq M_\Delta^2 - \frac{\lambda_4}{4} v_\Phi^2, \quad m_h^2 \simeq 2\lambda v_\Phi^2 \quad \text{and} \quad m_{H^0}^2 \simeq m_{A^0}^2 \simeq M_\Delta^2, \quad (31)$$

so their mass-squared differences can be written as

$$m_{H^\pm}^2 - m_{H^{\pm\pm}}^2 \approx m_{H^0/A^0}^2 - m_{H^\pm}^2 \approx \frac{\lambda_4}{4} v_\Phi^2. \quad (32)$$

Now we define two mass-splittings for the scalar fields $\{H^0, H^\pm\}$ and $\{H^+, H^\pm\}$ as

$$\delta m_1 = m_{H^0} - m_{H^\pm}, \quad \delta m_2 = m_{H^\pm} - m_{H^{\pm\pm}} \quad (33)$$

which could be further approximated to

$$\Delta m \equiv \delta m_{1,2} \approx \frac{\lambda_4}{8} \frac{v_\Phi^2}{M_\Delta}. \quad (34)$$

with the assumptions $v_\Delta \ll v_\Phi$ and $M_\Delta^2 \gg |\lambda_4| v_\Phi^2$. Hence we could express all the physical Higgs masses in terms of $m_{H^{\pm\pm}}$ and Δm only. The quartic coupling λ_4 between Φ and Δ should be small satisfying perturbative constraints at high energy below Planck scale. The mass splitting between singly and doubly charged multiplets of the triplet scalar $\Delta m = m_{H^\pm} - m_{H^{\pm\pm}}$ affects S, T and U parameters putting a stringent constraint as $|\Delta m| \lesssim 40 \text{ GeV}$ [68]. Depending on the value and sign of λ_4 we obtain three different spectra: (i) $\lambda_4 = 0$: $\Delta m \approx 0$ ($m_{H^{\pm\pm}} \simeq m_{H^\pm} \simeq m_{H^0/A^0}$), (ii) $\lambda_4 < 0$: $\Delta m < 0$ ($m_{H^{\pm\pm}} > m_{H^\pm} > m_{H^0/A^0}$) and (iii) $\lambda_4 > 0$: $\Delta m > 0$ ($m_{H^{\pm\pm}} < m_{H^\pm} < m_{H^0/A^0}$), respectively. The triplet scalar interacts with the SM gauge bosons and fermions. The partial decay widths of the doubly charged scalar into different modes taking $\Delta m \approx 0$ (degenerate scenario) into account can be given by

$$\Gamma(H^{\pm\pm} \rightarrow l_i^\pm l_j^\pm) = \frac{m_{H^{\pm\pm}}}{(1 + \delta_{ij}) 8\pi} \left| \frac{m_{ij}^\nu}{v_\Delta} \right|^2, \quad m_{ij}^\nu = Y_{\Delta_{ij}} v_\Delta / \sqrt{2}, \quad (35)$$

$$\Gamma(H^{\pm\pm} \rightarrow W^\pm W^\pm) = \frac{g^2 v_\Delta^2}{8\pi m_{H^{\pm\pm}}} \sqrt{1 - \frac{4}{r_W^2} [(2 + (r_W/2 - 1)^2)]}, \quad (36)$$

where $r_W = \frac{m_{H^{\pm\pm}}}{M_W}$ and m^ν represents the neutrino mass matrix with i, j as generation indices. For the case $\Delta m < 0$, one consider the additional decay mode as

$$\Gamma(H^{\pm\pm} \rightarrow H^\pm W^{\pm*}) = \frac{9g^4 m_{H^{\pm\pm}} \cos^2 \beta_\pm}{128\pi^3} G \left(\frac{m_{H^\pm}^2}{m_{H^{\pm\pm}}^2}, \frac{m_W^2}{m_{H^{\pm\pm}}^2} \right), \quad (37)$$

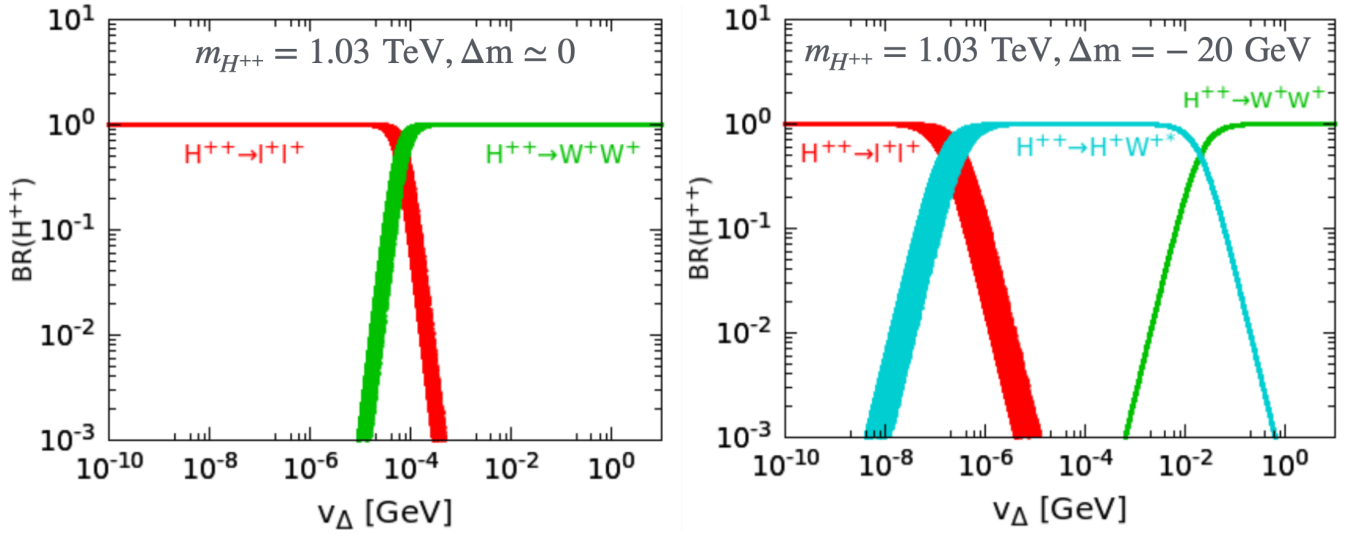


Figure 2. Branching ratios of $H^{\pm\pm}$ for $m_{H^{\pm\pm}} = 1.03$ TeV with $\Delta m \approx 0$ (left panel) and $\Delta m = -20$ GeV (right panel), respectively. We consider three decay mode of $H^{\pm\pm}$ into $\ell^\pm\ell^\pm$ (red), $W^\pm W^\pm$ (green) and $H^\pm W^{\pm*}$ (cyan), respectively. The decay mode $H^{\pm\pm} \rightarrow H^\pm W^{\pm*}$ is only open for $\Delta m < 0$ and further dominates in the region of intermediate v_Δ when Δm is relatively large.

where $\tan\beta_\pm = \frac{\sqrt{2}v_\Delta}{v_\Phi}$ and the functions $\lambda(x, y)$, $G(x, y)$ can be given by

$$\lambda(x, y) = (1 - x - y)^2 - 4xy, \quad (38)$$

$$G(x, y) = \frac{1}{12y} \left[2(-1+x)^3 - 9(-1+x^2)y + 6(-1+x)y^2 - 6(1+x-y)y\sqrt{-\lambda(x, y)} \right] \left\{ \tan^{-1} \left(\frac{1-x+y}{\sqrt{-\lambda(x, y)}} \right) + \tan^{-1} \left(\frac{1-x-y}{\sqrt{-\lambda(x, y)}} \right) \right\} - 3 \left(1 + (x-y)^2 - 2y \right) y \log x. \quad (39)$$

In Fig. 2, we show the branching ratios of $H^{\pm\pm}$ for $m_{H^{\pm\pm}} = 1.03$ TeV with $\Delta m \approx 0$ (left panel) and $\Delta m = -20$ GeV (right panel), respectively. For small Δm , depending on v_Δ , $H^{\pm\pm}$ dominantly decays either into same-sign dileptons for $v_\Delta \leq 10^{-4}$ GeV or gauge bosons for $v_\Delta > 10^{-4}$ GeV. On the other hand from the right panel of Fig. 2 with $\Delta m = -20$ GeV, the cascade mode $H^{\pm\pm} \rightarrow H^\pm W^{\pm*}$ dominate over the leptonic and diboson decay modes for an intermediate v_Δ . The doubly charged multiplet of the triplet scalar provide tightest constraints from the searches at the LHC. The collider searches strictly depend on v_Δ and Δm which governs the decay modes of the doubly charged multiplets, see Fig. 2. Assuming a degenerate scenario, bound on $m_{H^{\pm\pm}}$ can be obtained considering same sign leptonic decay of $H^{\pm\pm}$ at the 13 TeV LHC following Drell-Yan (DY) production. LHC has tested $H^{\pm\pm}H^\mp$ mode through s -channel W^\pm boson exchange followed by leptonic decay of the charged scalars. Combining these modes bounds on the triplet mass was obtained as $m_{H^{\pm\pm}} > 820$ GeV at 95% C.L. from CMS [35] and from DY process the bound is $m_{H^{\pm\pm}} > 1080$ GeV at 95% C.L. from ATLAS [40]. Using γ and Z exchange process in s -channel LEP provides a strong constrain as $m_{H^{\pm\pm}} > 97.3$ GeV [33] at 95% C.L. from doubly charged scalar multiplet pair production holding for $v_\Delta < 10^{-4}$ GeV only. For $v_\Delta > 10^{-4}$ GeV, $H^{\pm\pm}$ dominantly decays into $W^\pm W^\pm$ mode followed by the leptonic decay of the W bosons. Such modes have been studied by ATLAS providing a limit $m_{H^{\pm\pm}} \simeq 350$ GeV [41].

III. RESULTS AND DISCUSSIONS

We consider the minimal type-I seesaw scenarios to study two generations of heavy neutrinos. In this case we investigate a single electron(muon) final state in association with jets and neutrinos. In case of type-II seesaw scenario we study same-sign dilepton final state and doubly charged scalar multiplet production in association with Z boson and photon. We also study left-right asymmetry from the same-sign dilepton mode. We describe complete search strategies and results in the following way:

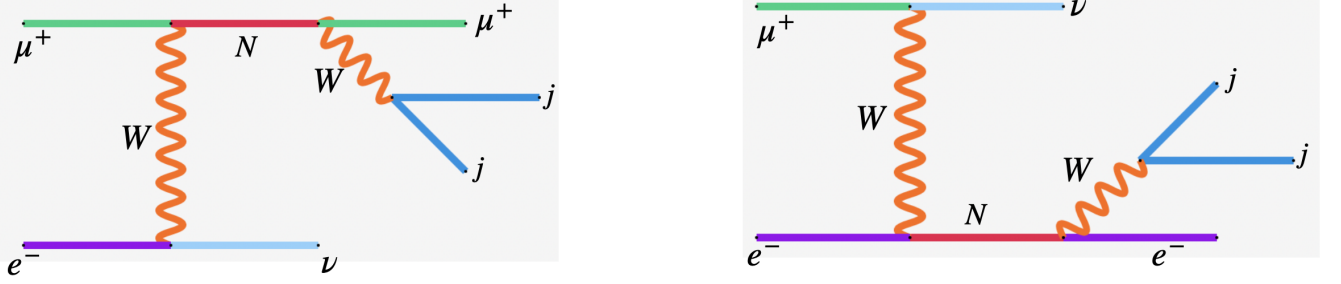


Figure 3. Heavy neutrino production processes in t -channel and its dominant decay in μ TRISTAN experiment. In this case we consider two generations of RHNs where one of them dominantly couples with muon(left) and the other dominantly couples with electron(right).

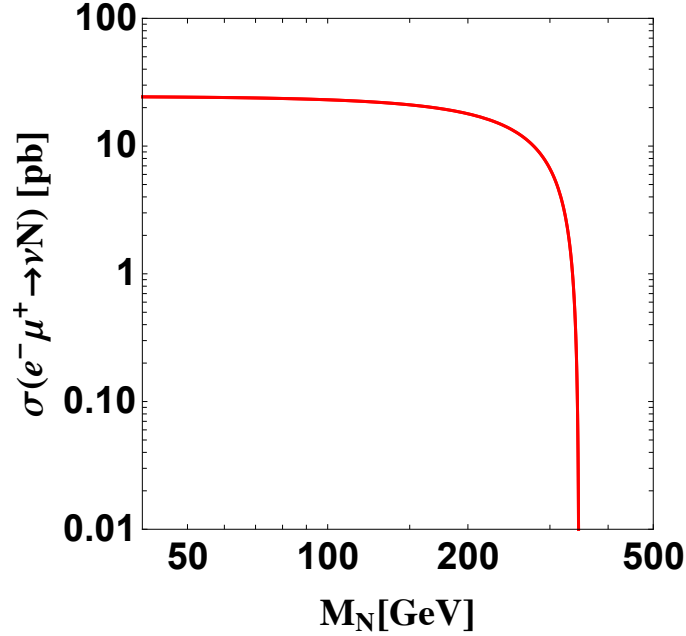


Figure 4. Heavy neutrino production cross section as a function of heavy neutrino mass in μ TRISTAN experiment at $\sqrt{s} = 346$ GeV center of mass energy normalized by the light-heavy mixing squared.

Heavy neutrino search

Depending on its flavor, the heavy neutrino can be produced in μ TRISTAN experiment through either of the processes shown in Fig. 3. To reduce the background, we only consider final states with hadronically decaying W boson. In this scenario we consider two generations of heavy neutrinos where first(second) generation dominantly couples with electron(muon). The differential scattering cross section for the t -channel process can be given by

$$\frac{d\sigma(\mu^+e^- \rightarrow N\nu)}{d\cos\theta} = (3.89 \times 10^8 \text{ pb}) \times \frac{(s - M_N^2)}{32\pi s^2} \times \left[\frac{g^4 \{(s - M_N^2)(1 \pm \cos\theta) \times (\frac{1}{2}s - \frac{1}{4}(s - M_N^2)(1 \mp \cos\theta))\}}{(\frac{1}{2}(s - M_N^2)(1 \mp \cos\theta) + M_W^2)^2 + \Gamma_W^2 M_W^2} \right] \quad (40)$$

where $g(= 0.65)$ is the $SU(2)$ gauge coupling, $M_W(= 80.4)$ GeV is the W boson mass and $\Gamma_W(= 2.4952)$ GeV is the total decay width of W boson for the heavy neutrino coming either from the muon or electron vertex, respectively. The production cross section of these heavy neutrinos in μ TRISTAN experiment at $\sqrt{s} = 346$ GeV center of mass energy are shown in Fig. 4. We find that the cross section falls sharply at the energy threshold. To obtain the signal cross section, we integrated over the scattering angle (θ_{sc}) in the range of $-0.95 < \cos\theta_{sc} < 0.95$. The cross sections for signal processes shown in Fig. 4 do not include the branching ratio of the heavy neutrino and the light-heavy mixing parameters have been set to unity. The branching ratios of heavy neutrinos could be found in Fig. 1.

To study the signal and SM backgrounds, we simulate corresponding events using the event generation package

MadGraph5_aMC@NLO [69] using the UFO model files generated by FeynRules [70]. The Pythia8 [71] is used to implement parton shower, hadronization and decay of the SM hadrons. The detector effects are simulated by Delphes [72] with the default ILC configuration card. The leading order cross sections of the generic SM backgrounds $\mu^+e^- \rightarrow e^+jj$ and μ^-jj are listed in Tab. I. While generating the background, the transverse momenta of the final state charged lepton and jets are required to be greater than 10 GeV and 20 GeV, respectively. To increase the signal significance, we

Process	σ [pb]
$\mu^+e^- \rightarrow e^+jj$	7.97×10^{-5}
$\mu^+e^- \rightarrow \mu^-jj$	8.42×10^{-5}

Table I. The leading order production cross section of generic SM backgrounds at $\sqrt{s} = 346$ in μ TRISTAN experiment.

will adopt the Gradient Boosted Decision Tree (GBDT) method [73] that takes into account several feature variables for signal and background discrimination. Only events that fulfill the following preselection cuts will be used in the training and testing of the GBDT: (1) exactly one charged lepton with $p_T(\ell^\pm) > 20$ GeV and $|\eta_\ell| < 2.5$; (2) either one or two jets with $p_T(j) > 20$ GeV, $|\eta_j| < 4.5$, and $m_{jj} \in [70, 90]$ GeV for two jets events¹; (3) missing transverse momentum $\cancel{E}_T < 60$ GeV. From those preselected events, we reconstruct several feature variables:

$$p^\mu(\ell^\pm), \cos(\theta_{\ell^\pm}), p^\mu(\ell jj), m_{\ell jj}. \quad (41)$$

The distributions for some of the feature variables are shown in Fig. 5. The GBDT method uses a 100 tree ensemble that requires a minimum training events in each leaf node of 1 and a maximum tree depth of three, with a learning rate of 0.1. It is training on benchmark signals with heavy neutrino masses in the range of [39, 300] GeV with a step size 14.5 GeV. For each mass, half of the preselected signal ($\sim 10^4$) and background ($\sim 10^4$) events are used in the training and testing of the GBDT respectively. To avoid overtraining, the sub-sample is required to be less than 0.8. After the training, the GBDT is able to assign a BDT score for each event. The score combines all discriminating abilities of the input feature variables, which can be used for signal and background discrimination. The BDT scores for signal and background are around unit and zero, respectively. In Fig. 6, the BDT score for a few benchmark signals and the corresponding backgrounds are shown. The signal and background are well-separated for each case, indicating the strong discriminating power of the GBDT. After the application of the kinematic cuts we write down the signal and background events in Tab. II for some benchmark heavy neutrino masses ($M_{N_{1(2)}}$) considering the decay of the heavy neutrinos in the ℓjj final state. After the application of all the kinematic cuts we estimate a 2σ

\sqrt{s} (GeV)	M_{N_1} (GeV)	Signal (S)		Background (B)	
		before cuts (pb)	after cuts (fb)	before cuts (fb)	after cuts (fb)
346	45	14.87	4.45	0.0842	0.016
	68	14.31	43.23	0.0842	3.12×10^{-4}
	97	14.50	83.15	0.0842	5.87×10^{-4}
	184	7.70	1046.13	0.0842	1.23×10^{-4}
	300	2.42	849.34	0.0842	3.44×10^{-4}
\sqrt{s} (GeV)	M_{N_2} (GeV)	Signal		Background	
		before cuts (pb)	after cuts (fb)	before cuts (fb)	after cuts (fb)
346	45	14.87	47.58	0.0797	0.013
	68	14.31	1045.93	0.0797	1.27×10^{-4}
	97	14.50	523.40	0.0797	4.68×10^{-4}
	184	7.70	2305.81	0.0797	1.31×10^{-4}
	300	2.42	2236.41	0.0797	1.94×10^{-4}

Table II. Signal normalized by light-heavy mixing squared and SM background cross sections before and after cuts for several benchmark points of the heavy neutrino masses.

contour on the $M_{N_{1(2)}} - |V_{e(\mu)N_{1(2)}}|^2$ plane solving the following equation

$$\sigma = \frac{S \times |V_{e(\mu)N_{1(2)}}|^2}{\sqrt{S \times |V_{e(\mu)N_{1(2)}}|^2 + B}}, \quad (42)$$

¹ The one jet final state corresponds to a boosted hadronically decaying W boson.

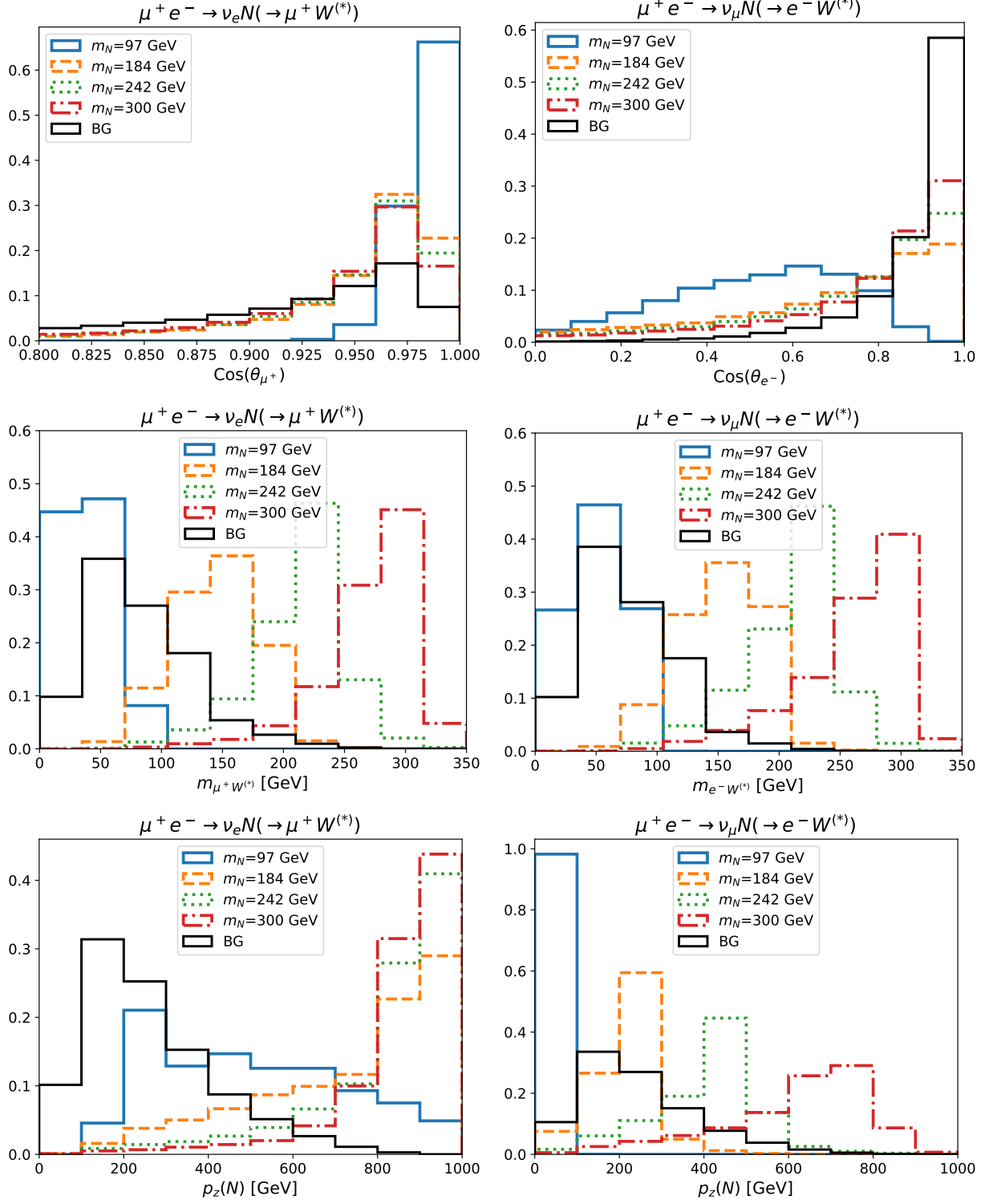


Figure 5. Feature variables that input to the BDT from top to bottom: $\cos\theta$ of μ/e , invariant mass and longitudinal momentum of the reconstructed heavy neutrino. Left panels: muonic flavor heavy neutrino; Right panels: electronic flavor heavy neutrino.

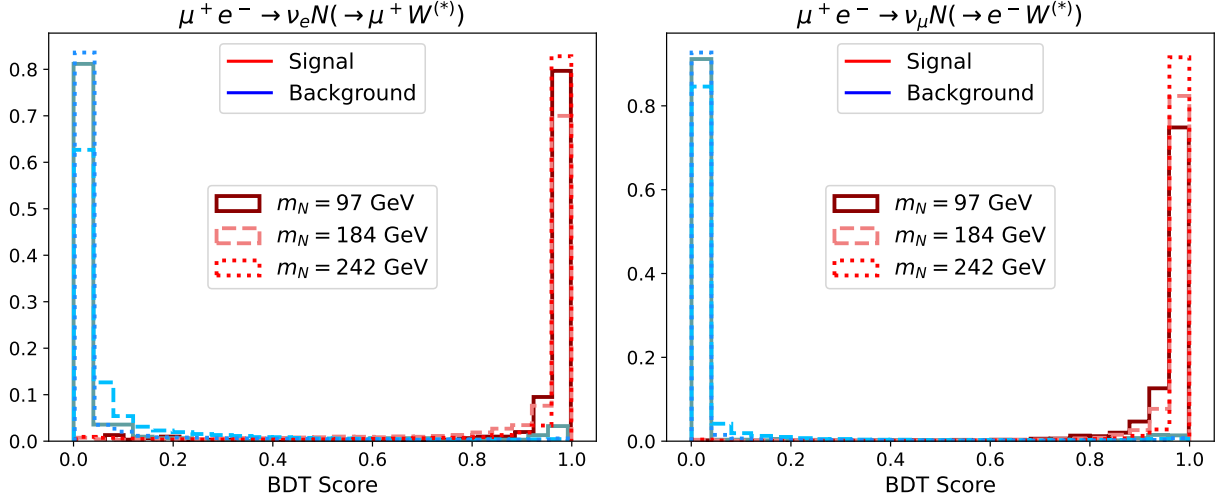


Figure 6. The BDT score for a few benchmark signals and the corresponding backgrounds.

where S and B stands for signal and corresponding background events, respectively at 1 ab^{-1} luminosity. Corresponding estimated bounds for electron and muon bounds are shown in Fig. 7 which are represented by orange dashed line for the first (upper panel) and second (lower panel) generation cases. We show shaded regions in these figures which are already ruled out by different existing searches. From our analysis we find that in case of the first generation heavy neutrinos, prospective limits could be stronger than existing bounds from prompt heavy neutrino searches from CMS [74, 75] and EWPD [76–78] for $77 \text{ GeV} \leq M_{N_1} \leq 315 \text{ GeV}$. We find that for $93 \text{ GeV} \leq M_{N_1} \leq 295 \text{ GeV}$, mixing could vary $4.2 \times 10^{-6} \leq |V_{eN_1}|^2 \leq 10^{-5}$. In addition to that, we estimate prospective limits on the light-heavy mixing square for the second generation heavy neutrino which could provide stronger limits compared to prompt heavy neutrino searches from CMS [74, 75] (gray solid) and EWPD (cyan solid(dashed)) for electron(muon)[76–78] for $61.5 \text{ GeV} \leq M_{N_2} \leq 321 \text{ GeV}$. We find that for $88 \text{ GeV} \leq M_{N_2} \leq 304 \text{ GeV}$, mixing could vary around $2.0 \times 10^{-6} < |V_{\mu N_2}|^2 \leq 10^{-5}$. These limits could be probed in future.

We compare the prospective bounds with existing results from a variety of experiments represented by the gray shaded region in Fig. 7. Bounds from the same sign di-lepton (SSDL) search by ATLAS and CMS experiments at $\sqrt{s} = 8 \text{ TeV}$ LHC are shown by the red dashed and dotted lines from [79, 80]. Experimental bounds from L3 detector of the LEP experiment are shown by light green dot dashed line from [81] in Fig. 7 (upper panel). Bounds from $\sqrt{s} = 13 \text{ TeV}$ LHC using the SSDL searches from CMS [20] using cyan dot-dashed and trilepton searches from ATLAS [82] using cyan dashed and CMS [19] brown dot dashed lines, respectively. Bounds obtained from the prompt (Pr) and long-lived (LL) heavy neutrinos searches from the DELPHI [83] experiment are represented by black dot dashed and dashed lines, respectively. Bounds on the mixing using long-lived particle (LLP) searches for Majorana type heavy neutrinos from the CMS [22] are shown by purple dashed line in the upper panel of Fig. 7. Conservative limits on Majorana type heavy neutrino mixing from the meson decay are shown by light green dashed line following [84]. Displaced vertex (DV) searches in ATLAS from Majorana type heavy neutrinos are taken from [85, 86] where bounds are shown for single flavor (1F) case with normal hierarchy (NH) and inverted hierarchy (IH) scenarios, respectively by blue dotted, green dashed, magenta dotted and red dot dashed lines. We show corresponding CMS bounds for displaced vertex from Majorana type heavy neutrinos by pink dot dashed line [75]. We also estimate bounds on the light-heavy mixing from the top quark decay into heavy Majorana neutrinos shown by light green solid line in the shaded region [87]. Limits on the light-heavy mixing due to the second generation heavy neutrino studying the vector boson fusion process from ATLAS (VBF-ATLAS13, VBF-ATLAS13-2)[86, 88, 89] and CMS (SSDM(W)) [21] are shown by different yellow lines in the gray shaded region. Prospective bounds obtained from the future electron positron circular collider (FCC-ee) are shown by the dashed Magenta line from [90] in the upper panel of Fig. 7. Prospective limits on the light-heavy mixing from the SHiP experiment are shown by the darker red dot dashed line from [91, 92] and those from the NA62 experiments are shown by darker red dashed line [93–96], respectively. Prospective limits from MATHUSLA at FCC-hh for the W/Z boson decays for MATHUSLA surface version(M-WZ-FCC-hh(S)) and forward version(M-WZ-FCC-hh(F)) are shown by orange dashed and dotted lines, respectively. Similarly prospective limits for the heavy neutrinos produced from the W/Z boson decays at high luminosity LHC (HL-LHC) are represented by M-HL-LHC-WZ and these bounds are shown by solid orange line in the upper panel of Fig. 7 for the first generation heavy neutrinos. Bounds on light-heavy neutrino mixing obtained from the B/D meson

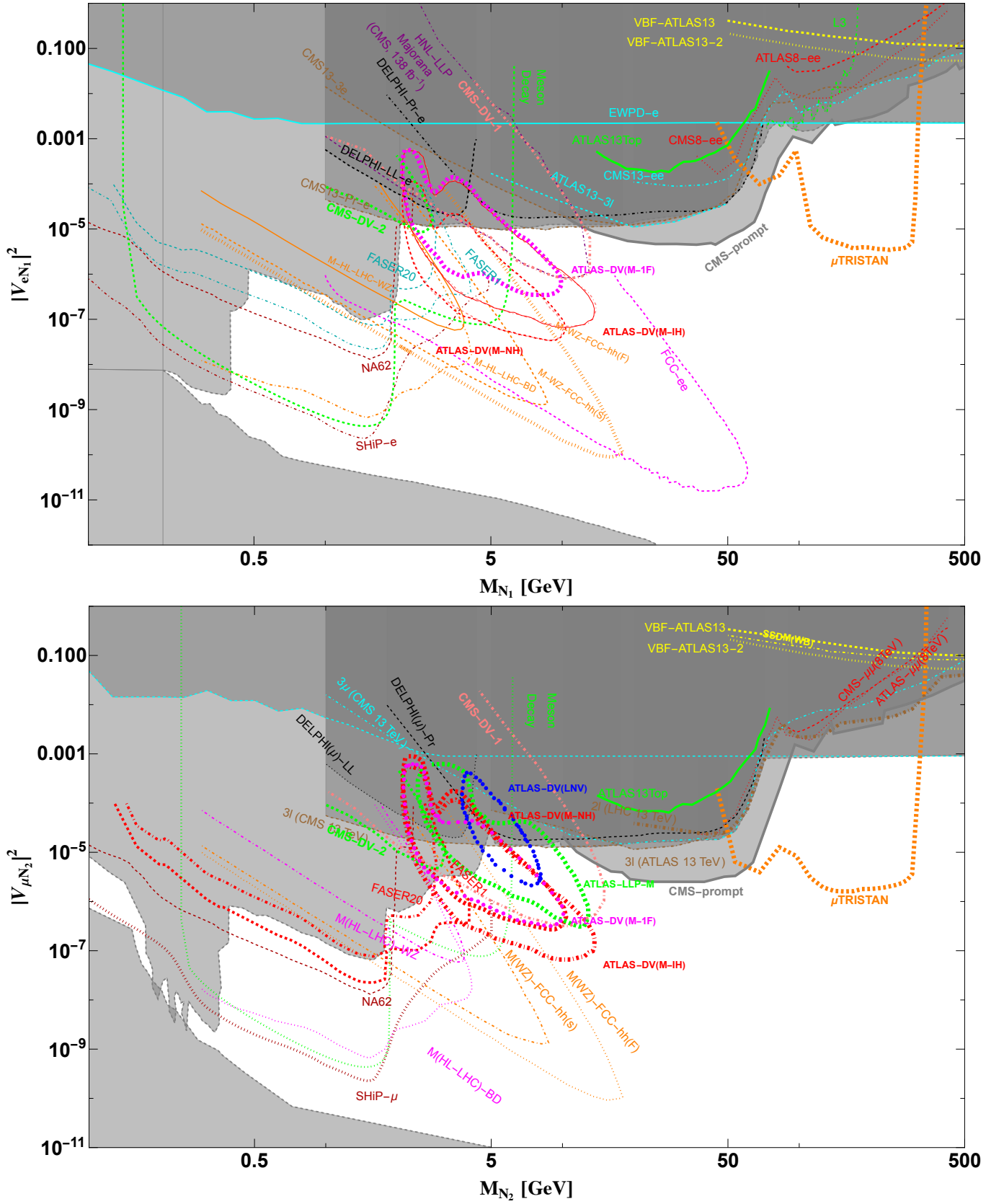


Figure 7. Limits on light-heavy mixing with respect to first (upper) and second (lower) generation heavy neutrino masses from μ TRISTAN experiment (orange dashed, thick) at $\sqrt{s} = 346$ GeV and 1 ab^{-1} luminosity and compared with prospective bounds from FASER, MATHUSLA, NA62, FCC-ee and SHiP analyses. Shaded regions are already ruled out by different existing experimental searches. See text for details.

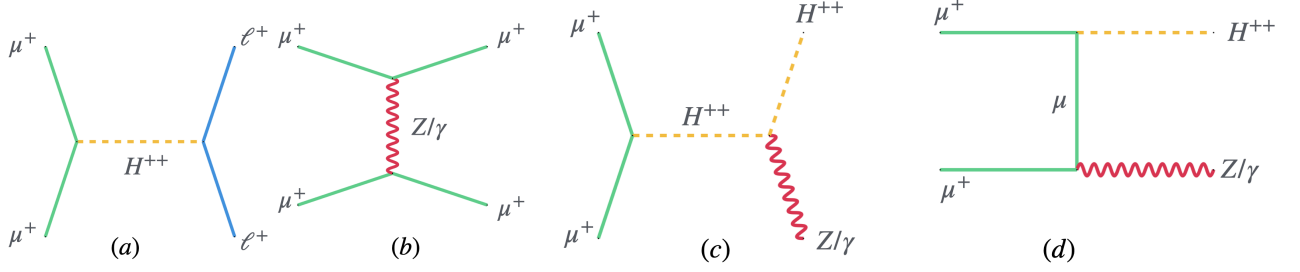


Figure 8. Doubly charged scalar multiplet (H^{++}) mediated $\mu^+\mu^+ \rightarrow \ell^+\ell^+$ processes in (a) and the SM backgrounds (γ, Z) in (b) in μ TRISTAN experiment within type-II seesaw framework. Feynman diagrams for $\mu^+\mu^+ \rightarrow H^{++}Z/\gamma$ process are shown in (c) and (d) followed by the decay $H^{++} \rightarrow \ell^+\ell^+$ which could be tested in μ TRISTAN experiment at $\sqrt{s}=2$ TeV.

decays are represented by M-HL-LHC-BD and shown by thick orange dot dashed line [97]. Prospective bounds on the light-heavy neutrino mixing obtained from the FASER collaboration with detector radius 20 cm (1 m) are shown by the darker cyan dashed(dot dashed) line marked as FASER20 (FASER1) respectively from [98, 99]. Lower part of the shaded region consists of the exclusion limits obtained from experiments like CHARM, JNIR, PS191 [100–104] and theoretically estimated bounds from BBN and seesaw [11, 105–109] scenarios in counter-clockwise direction from below.

Triplet scalar search

We consider the type-II seesaw scenario where doubly charged component of the $SU(2)$ scalar triplet could play a crucial role in $\mu^+\mu^+$ collision of the proposed μ TRISTAN collider using [69]. In this case we consider a center of mass energy $\sqrt{s} = 2$ TeV with a luminosity of 1 ab^{-1} . We consider two scenarios for type-II seesaw where we produce same sign dilepton following $\mu^+\mu^+ \rightarrow \ell_i^+\ell_j^+$ scenario where s -channel and the SM background could be obtained from the t -channel $\mu^+\mu^+ \rightarrow \mu^+\mu^+$ process using Z/γ exchange. Corresponding Feynman diagrams are given in Fig. 8. Total production cross section of $\mu^+\mu^+ \rightarrow \ell_i^+\ell_j^+$ ($\neq \mu^+\mu^+$) signal process can be given by

$$\sigma(\mu^+\mu^+ \rightarrow \ell_i^+\ell_j^+) = \frac{|Y_{\Delta}^{\mu\mu}Y_{\Delta}^{ij}|^2}{4\pi(1 + \delta_{ij})} \frac{s}{(s - m_{H^{\pm\pm}}^2)^2 + m_{H^{\pm\pm}}^2\Gamma_{H^{\pm\pm}}^2}, \quad (43)$$

neglecting initial and final state lepton masses. Here $\sqrt{s} = 2$ TeV, δ_{ij} is Kronecker delta vanishing for leptons of different kind, giving unity for same type leptons and $\Gamma_{H^{\pm\pm}}$ is the total decay width of $H^{\pm\pm}$. We consider a luminosity of 1 ab^{-1} to estimate number of events for the signal and background. In Fig. 9 we show the number of events for the process for same sign dilepton mediated by H^{++} as a function of $m_{H^{++}}$ which attains a maximum at $m_{H^{++}} = 2$ TeV. In this analysis we generate the signal and background events with transverse momentum of the leptons as $p_T^{\ell} > 400$ GeV and $E_T^{\text{max}} < 10$ GeV. We find that generic SM backgrounds are very large for $\mu^+\mu^+$ final state as a result we did not show the results for this final state. However, for the other combinations of the signal events like $e^+\mu^+$, $\mu^+\tau^+$, $e^+\tau^+$ and $\tau^+\tau^+$ the number of signal events are large compared to the almost negligible amount of generic SM backgrounds. From these cases we find it is difficult to distinguish between the NO and IO cases of the neutrino mass hierarchy given in the left and right sides of the top and middle panels of Fig. 9. In the bottom panel of Fig. 9 we show the events for the $\mu^+\mu^+ \rightarrow e^+e^+$ process for NO and IO scenarios as a function of $m_{H^{++}}$. We find that the number of events for NO case are different from the IO case where events for IO case could be at least three to four orders of magnitude larger than the NO case. In the lower right panel of Fig. 9 we show the number of events for $\mu^+\mu^+ \rightarrow e^+e^+$ process as a function of the lightest light neutrino mass (m_{lightest}) fixing $m_{H^{++}} = 1.03$ TeV. We find that for $m_{\text{lightest}} < 0.01$ eV numbers of events for the NO and IO scenarios become nearly two orders of magnitude different. Depending on neutrino oscillation data IO case could provide $\mathcal{O}(100)$ events which could be $\mathcal{O}(10)$ events for the luminosity 100 fb^{-1} . In this case number of events for NO case is small for 1 ab^{-1} that will be lower for 100 fb^{-1} luminosities. Therefore $\mu^+\mu^+ \rightarrow e^+e^+$ process mediated by H^{++} can be tested in the μ TRISTAN experiment to probe IO of the neutrino mass generation mechanism. In this analysis v_{Δ} and $m_{H^{++}}$ are taken in such a way that the branching ratios of the LFV decay mode $\mu \rightarrow e\gamma$ and $\mu \rightarrow 3e$ are satisfied by the experimental limits $\text{BR}(\mu \rightarrow e\gamma) = 4.2 \times 10^{-13}$ and $\text{BR}(\mu \rightarrow 3e) = 10^{-12}$ [110, 111], respectively. The neutrino oscillation parameters are varied within their allowed 3σ range [31] whereas the Majorana phases (ϕ_1, ϕ_2) are set to be zero. The gray shaded region in the bottom right panel of Fig. 9 is excluded from the combined analysis of CMB+BAO [112]. We found

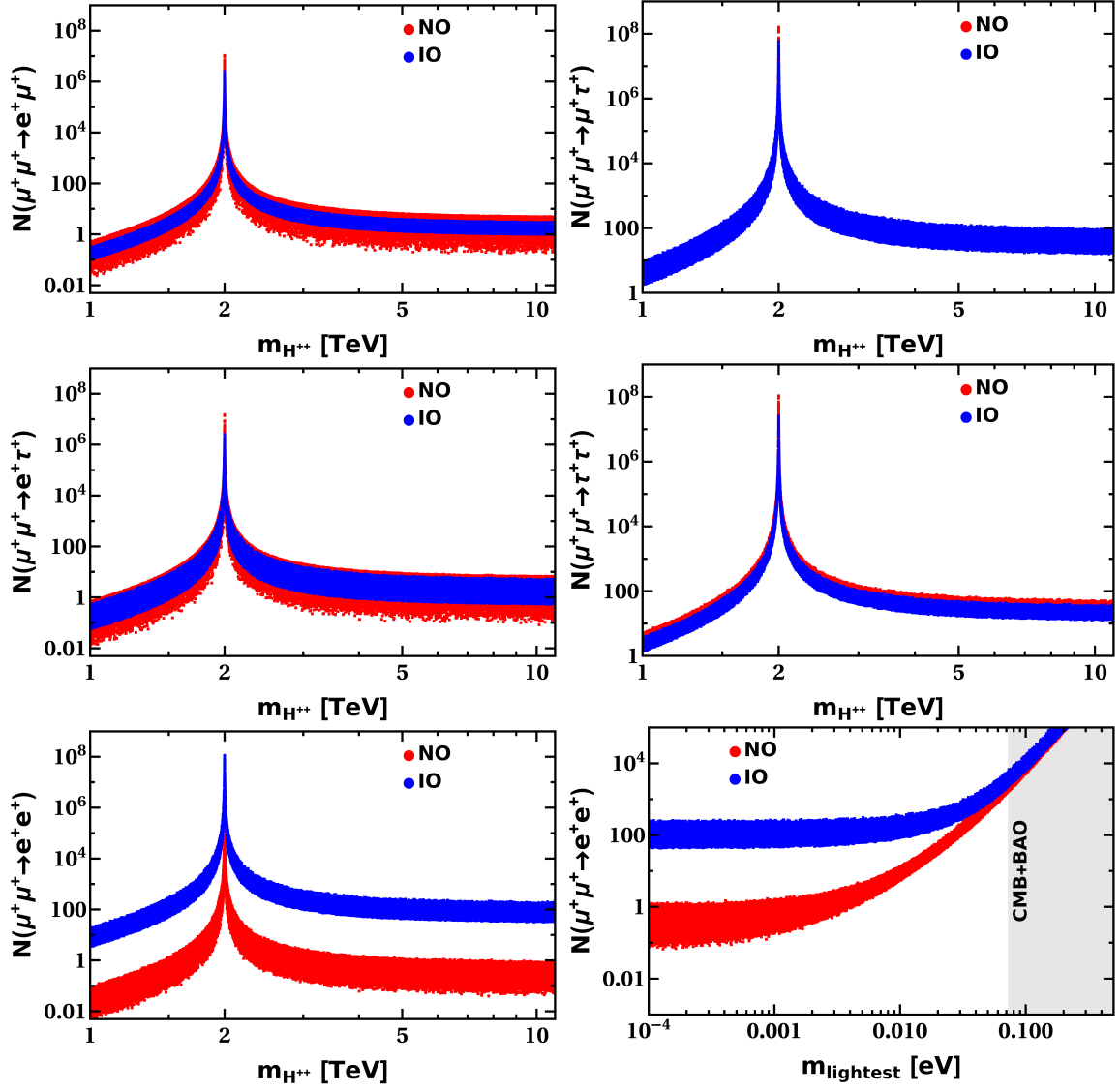


Figure 9. The number of the events for the processes $\mu^+\mu^+ \rightarrow e^+\mu^+$ (upper left), $\mu^+\mu^+ \rightarrow \mu^+\tau^+$ (upper right), $e^+\tau^+$ (middle left), $\tau^+\tau^+$ (middle right) and e^+e^+ (bottom) as a function of $m_{H^{++}}$ for $m_{\text{lightest}} = 0$. We show the number of events for $\mu^+\mu^+ \rightarrow e^+e^+$ case as function of lightest neutrino mass for $m_{H^{++}} = 1.03$ TeV in μ TRISTAN collider considering $\sqrt{s} = 2$ TeV and luminosity as $\mathcal{L} = 1 \text{ ab}^{-1}$ assuming v_Δ and $m_{H^{++}}$ to be taken in such a way that the branching ratios of the LFV processes $\mu \rightarrow e\gamma$ and $\mu \rightarrow 3e$ are satisfied by the experimental limits $\text{BR}(\mu \rightarrow e\gamma) = 4.2 \times 10^{-13}$ and $\text{BR}(\mu \rightarrow 3e) = 10^{-12}$ [110, 111], respectively. The neutrino oscillation parameters are varied within their allowed 3σ range [31] whereas the Majorana phases (ϕ_1, ϕ_2) are set to be zero. The gray shaded region in the bottom right panel is excluded from the combined analysis of CMB+BAO [112].

that the generic SM background is negligibly small, therefore depending on $m_{H^{++}}$ and m_{lightest} IO scenarios could be observed at the μ TRISTAN experiment with at least 3σ significance or more considering e^+e^+ final state with luminosity varying between 100 fb^{-1} to 1 ab^{-1} .

We study another production mode of H^{++} following $\mu^+\mu^+ \rightarrow H^{++}\gamma/Z$ and the corresponding Feynman diagrams are given in Fig. 8. We first consider the scenario $\mu^+\mu^+ \rightarrow H^{++}\gamma \rightarrow e^+e^+\gamma$ to generate events using MadGraph[69]. In this analysis we apply the kinematic cuts for the photon as $p_T^\gamma > 50$ GeV and lepton as $p_T^e > 400$ GeV, $E_T^{\text{max}} < 10$ GeV, respectively. After cuts, signal events become almost half of the events before cut for the final state $e^+e^+\gamma$ where e^+e^+ will be produced from H^{++} decay. The generic SM background reduces to 10^{-11} pb after the application of kinematic cuts from the cross section 3.7451×10^{-5} pb obtained before application of kinematic cuts. As a result after cuts SM background becomes negligible. These SM backgrounds could be large for $\mu^+\mu^+$ mode. Therefore we do not consider $H^{++} \rightarrow \mu^+\mu^+$ mode. In the same line we generate events for $\mu^+\mu^+ \rightarrow H^{++}Z \rightarrow e^+e^+jj$ considering hadronically

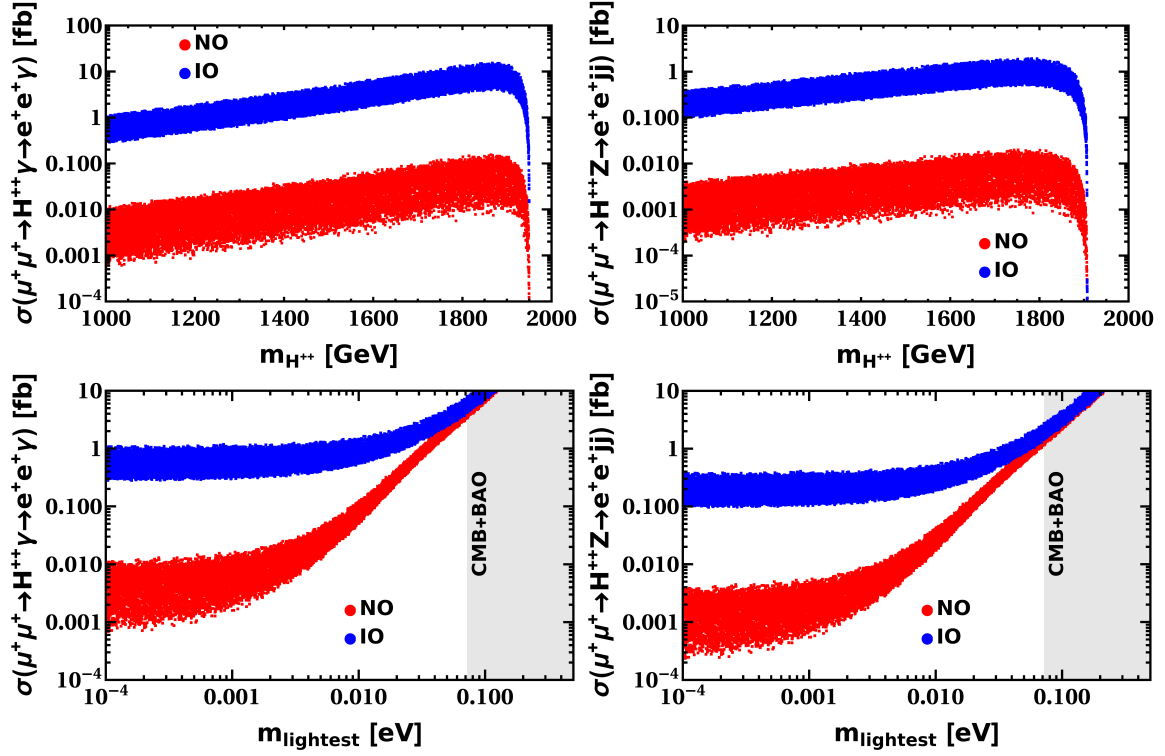


Figure 10. Cross sections of $\mu^+\mu^+ \rightarrow e^+e^+\gamma$ (upper left panel) and e^+e^+jj (upper right panel) processes after cut with $\sqrt{s} = 2$ TeV and $m_{\text{lightest}} = 0$ in the μ TRISTAN experiment. Fixing $m_{H^{++}} = 1.03$ TeV distinction between NO and IO cases are shown (bottom panel) as a function of m_{lightest} . We assume v_Δ and $m_{H^{++}}$ to be taken in such a way that the branching ratios of the LFV processes $\mu \rightarrow e\gamma$ and $\mu \rightarrow 3e$ are satisfied by the experimental limits $\text{BR}(\mu \rightarrow e\gamma) = 4.2 \times 10^{-13}$ and $\text{BR}(\mu \rightarrow 3e) = 10^{-12}$ [110, 111], respectively. The neutrino oscillation parameters are varied within their allowed 3σ range [31] whereas the Majorana phases (ϕ_1, ϕ_2) are set to be zero. The gray shaded region in the bottom right panel is excluded from the combined analysis of CMB+BAO [112].

decaying Z boson due to larger branching ratio over leptonic mode. In addition to that, we do not consider all muon final states due to large SM background. To analyze these signal and SM background events we apply kinematic cuts as $p_T^\gamma > 50$ GeV, $p_T^j > 400$ GeV, $p_T^\mu > 20$ GeV, $E_T^{\text{max}} < 10$ GeV. Signal events after cut is almost 84% of the events before cut. Applying these cuts we find that the generic SM background reduces to 10^{-12} pb from the cross section 7.52×10^{-6} pb before cuts. We show the cross section of these processes as a function of $m_{H^{++}}$ in the upper panel of Fig. 10 after applying kinematic cuts. Depending on triplet mass, the cross section of $e^+e^+\gamma$ final state could vary between 1 fb to 15 fb for $1 \text{ TeV} \leq m_{H^{++}} \leq 1.95 \text{ TeV}$ in the IO case whereas that could vary between 0.01 fb to 0.1 fb in the NO case for the same range of $m_{H^{++}}$ which could provide distinguishable number of events for the neutrino mass orderings if luminosity varies between 100 fb^{-1} to 1 ab^{-1} . On the other hand cross sections for the e^+e^+jj process could vary between 0.1 fb to 2 fb for $1 \text{ TeV} \leq m_{H^{++}} \leq 1.9 \text{ TeV}$ for the IO scenario whereas that for the NO scenario is roughly one order of magnitude small. This final state can also produce significantly large difference between the neutrino mass orderings if luminosity varies between 100 fb^{-1} to 1 ab^{-1} . As a result depending on $m_{H^{++}}$ and m_{lightest} we could distinguish between the NO and IO cases at least 3σ significance or more if the luminosity varies between 100 fb^{-1} to 1 ab^{-1} . In the lower panel of Fig. 10 we show difference between the cross sections of the same final states as a function of m_{lightest} for the NO and IO cases and the difference between these two orderings of the neutrino mass comes prominent for $m_{\text{lightest}} \leq 0.01$ eV. Depending on luminosity between 100 fb^{-1} to 1 ab^{-1} the significance of finding different neutrino mass hierarchies could be at least 3σ or more.

In the context of type-II seesaw scenario we also consider the $\mu^+\mu^+ \rightarrow \ell^+\ell^+$ process where BSM process will be produced through H^{++} in s -channel and the SM case will be mediated by Z boson and γ in t -channel, respectively. Corresponding Feynman diagrams are given in Fig. 8. Here we consider polarized cross sections at the μ TRISTAN experiment considering center of mass energy as $\sqrt{s} = 2$ TeV with 1 ab^{-1} luminosity and discuss left-right asymmetry in use of the method in ref. [113]. The scattering process is given by

$$\mu^+(k_1, \sigma_1) + \mu^+(k_2, \sigma_2) \rightarrow \ell^+(k_3, \sigma_3) + \ell^+(k_4, \sigma_4), \quad (44)$$

where σ_i indicate helicity and $\ell = \{e, \mu, \tau\}$. In addition to the SM interactions we take into account doubly charged scalar exchanging interaction described by effective operator

$$\mathcal{L}_{\text{eff}} = \frac{(Y_{\Delta}^{\dagger} Y_{\Delta})_{\mu\ell}}{2m_{H^{++}}^2} (\bar{\mu}\gamma^{\mu} P_L \mu) (\bar{\ell}\gamma_{\mu} P_L \ell). \quad (45)$$

Squared helicity amplitudes $|\mathcal{M}_{\{\sigma_i\}}|^2 = |\mathcal{M}(\sigma_1\sigma_2\sigma_3\sigma_4)|^2$ for the $\mu^+\mu^+ \rightarrow \mu^+\mu^+$ process are calculated as

$$|\mathcal{M}(+ - + -)|^2 = |\mathcal{M}(- + - +)|^2 = s^2 (1 + \cos\theta)^2 \left[\frac{e^2}{t} + \frac{g_L g_R}{t_Z} \right]^2, \quad (46)$$

$$|\mathcal{M}(+ - - +)|^2 = |\mathcal{M}(- + + -)|^2 = s^2 (1 - \cos\theta)^2 \left[\frac{e^2}{u} + \frac{g_L g_R}{u_Z} \right]^2, \quad (47)$$

$$|\mathcal{M}(+ + + +)|^2 = 4s^2 \left[e^2 \left(\frac{1}{t} + \frac{1}{u} \right) + g_R^2 \left(\frac{1}{t_Z} + \frac{1}{u_Z} \right) \right]^2, \quad (48)$$

$$|\mathcal{M}(- - - -)|^2 = 4s^2 \left[e^2 \left(\frac{1}{t} + \frac{1}{u} \right) + g_L^2 \left(\frac{1}{t_Z} + \frac{1}{u_Z} \right) - \frac{(Y_{\Delta}^{\dagger} Y_{\Delta})_{\mu\mu}}{m_{H^{++}}^2} \right]^2, \quad (49)$$

where $g_L = e(-1/2 + s_W^2)/(s_W c_W)$, $g_R = es_W/c_W$, $s = (k_1 + k_2)^2 = (k_3 + k_4)^2$, $t = (k_1 - k_3)^2 = (k_2 - k_4)^2 = -s(1 - \cos\theta)/2$, $u = (k_1 - k_4)^2 = (k_2 - k_3)^2 = -s(1 + \cos\theta)/2$, $u_Z = u - m_Z^2 + im_Z\Gamma_Z$, $t_Z = t - m_Z^2 + im_Z\Gamma_Z$, and $\cos\theta$ is the scattering polar angle. For $\mu^+\mu^+ \rightarrow e^+e^+(\tau^+\tau^+)$ process, we do not have the SM contribution and the amplitude is only

$$|\mathcal{M}'(- - - -)|^2 = 4s^2 \left[\frac{(Y_{\Delta}^{\dagger} Y_{\Delta})_{\mu e(\tau)}}{m_{H^{++}}^2} \right]^2. \quad (50)$$

Here we write differential cross-section for purely-polarized initial-state as

$$\frac{d\sigma_{\sigma_1\sigma_2}}{d\cos\theta} = \frac{1}{32\pi s} \sum_{\sigma_3, \sigma_4} |\mathcal{M}_{\{\sigma_i\}}|^2. \quad (51)$$

For realistic case, we consider partially-polarized initial-state with the degree of polarization P_{μ^+} for the μ^+ beams, and the polarized cross section is given as

$$\begin{aligned} \frac{d\sigma(P_{\mu^+}, P_{\mu^+})}{d\cos\theta} &= \frac{1 + P_{\mu^+}}{2} \frac{1 + P_{\mu^+}}{2} \frac{d\sigma_{++}}{d\cos\theta} + \frac{1 + P_{\mu^+}}{2} \frac{1 - P_{\mu^+}}{2} \frac{d\sigma_{+-}}{d\cos\theta} \\ &+ \frac{1 - P_{\mu^+}}{2} \frac{1 + P_{\mu^+}}{2} \frac{d\sigma_{-+}}{d\cos\theta} + \frac{1 - P_{\mu^+}}{2} \frac{1 - P_{\mu^+}}{2} \frac{d\sigma_{--}}{d\cos\theta}. \end{aligned} \quad (52)$$

For μ TRISTAN, we consider the following right-handed and left-handed cases:

$$\frac{d\sigma_R}{d\cos\theta} = \frac{d\sigma(P_{\mu^+} = -0.8, P_{\mu^+} = -0.8)}{d\cos\theta}, \quad (53)$$

$$\frac{d\sigma_L}{d\cos\theta} = \frac{d\sigma(P_{\mu^+} = 0.8, P_{\mu^+} = 0.8)}{d\cos\theta}. \quad (54)$$

To study the sensitivity to the doubly-charged scalar effects on $\mu^+\mu^+ \rightarrow \mu^+\mu^+$ scattering process, we consider the left-right (LR) asymmetry defined by

$$A_{LR} = \frac{N_R - N_L}{N_R + N_L}, \quad (55)$$

where

$$N_{L(R)} = \mathcal{L} \cdot \int_{-0.95}^{0.95} d\cos\theta \frac{d\sigma_{L(R)}}{d\cos\theta}, \quad (56)$$

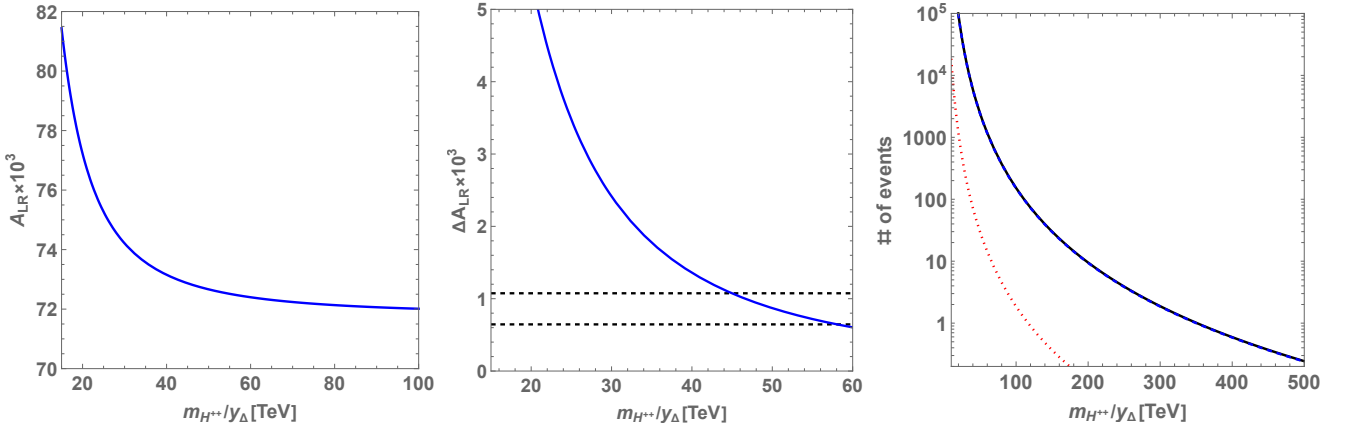


Figure 11. Left right asymmetry (left most panel) and the deviation (middle panel) from the SM at 3σ (lower black dashed line) and 5σ (upper black dashed line) significance as a function of $m_{H^{++}}/Y_{\Delta}$ for $\mu^+\mu^+ \rightarrow \mu^+\mu^+$ process in μ TRISTAN experiment at $\sqrt{s} = 2$ TeV at 1 ab^{-1} luminosity. In the right most panel we show total number of events for e^+e^+ and $\tau^+\tau^+$ final states for left (N_L) and right (N_R) polarizations represented by red dotted and blue-black solid lines.

where $\mathcal{L} = 1 \text{ ab}^{-1}$ is the luminosity we consider in this analysis. To estimate total cross sections we integrate over the range $-0.95 \leq \cos \theta \leq 0.95$ of the scattering angle. We also consider a statistical error of the asymmetry given by

$$\delta A_{LR} = \sqrt{\frac{1 - A_{LR}^2}{N_R + N_L}}. \quad (57)$$

The sensitivity to the new physics scenario is estimated at some confidence level ($x \sigma$) by requiring

$$|A_{LR}(\text{SM} + \delta^{++}) - A_{LR}(\text{SM})| \geq x \times \delta A_{LR}(\text{SM}), \quad (58)$$

where $A_{LR}(\text{SM})[\delta A_{LR}(\text{SM})]$ can be obtained by considering the limit $m_{H^{++}} \rightarrow \infty$. For $\mu^+\mu^+ \rightarrow e^+e^+(\tau^+\tau^+)$ process, we simply consider number of event $N_{L,R}$ since there is no SM contribution. The corresponding results are shown in the left and middle panels of Fig. 11 where we estimate LR asymmetry (A_{LR}) for the $\mu^+\mu^+ \rightarrow \mu^+\mu^+$ process and its corresponding deviation (ΔA_{LR}) from the SM as a function of $m_{H^{++}}/Y_{\Delta}$. We find that the deviation could be probed by the μ TRISTAN collider at 3σ (upper black dashed line) and 5σ (lowe black dashed line) levels with $\sqrt{s} = 2$ TeV and $\mathcal{L} = 1 \text{ ab}^{-1}$ for $m_{H^{++}}/Y_{\Delta} > 45$ TeV. In the right most panel of Fig. 11 we show the number of events for left (N_L) and right (N_R) polarizations represented by red dotted and blue-black solid lines obtained from e^+e^+ and $\tau^+\tau^+$ final states as a function of $m_{H^{++}}/Y_{\Delta}$ where there is no SM background. We find that $N_R > N_L$ by two orders of magnitude through out the range of $m_{H^{++}}/Y_{\Delta}$ under consideration. In μ TRISTAN experiment we could probe a high scale of triplet mass though sizable left-right asymmetry for different same sign dilepton mode and deviation of left-right asymmetry from the SM scenario for e^+e^+ final state.

IV. CONCLUSIONS

We study two different tree level seesaw scenarios, namely, minimal TeV scale type-I and type-II seesaw models in proposed μ TRISTAN collider at $\sqrt{s} = 346$ GeV and 2 TeV considering μ^+e^- and $\mu^+\mu^+$ collisions. In case of μ^+e^- collider we study the productions of first and second generation heavy RHNs in association with light neutrinos. These heavy RHNs dominantly couple with electron and muon, respectively through high-heavy neutrino mixing. These heavy neutrinos decay through the dominant mode of a charged lepton and jets providing a single lepton, missing momentum and jets. Generating events for the signal and generic SM backgrounds we estimate prospective limits on the light-heavy mixing angles of these heavy neutrinos at 1 ab^{-1} luminosity at 2σ significance. We find that mixing for the first generation heavy neutrino mixing could be probed between $4.2 \times 10^{-6} \leq |V_{eN_1}|^2 \leq 10^{-5}$ for $93 \text{ GeV} \leq M_{N_1} \leq 295 \text{ GeV}$ which is two orders of magnitude stronger than EWPD limits. Similarly for the second generation of the heavy neutrino mixing could be probed between $2.0 \times 10^{-6} < |V_{\mu N_2}|^2 \leq 10^{-5}$ for $88 \text{ GeV} \leq M_{N_2} \leq 304 \text{ GeV}$ which is also nearly two orders of magnitude stronger than the limits obtained from EWPD at 1 ab^{-1} luminosity. In addition to that we have studied same sign dilepton production from the doubly charged scalar induced interactions from the type-II seesaw scenario. We estimated that such a scenario could depend on neutrino oscillation data and

hence on neutrino mass hierarchy. Generating signal events for different final states involving photon, same sign lepton and jets we find that it could be possible to differentiate between the NO and IO. Avoiding purely muons in the final state we find that purely two positron final state could provide nearly two orders of magnitude more events if inverted hierarchy of the neutrino mass is considered compared to the normal hierarchy scenario. Final states with unlike flavor and same sign dilepton can not distinguish between the neutrino mass hierarchies at 1 ab^{-1} luminosity. On the other hand if we consider two positron final state in association with photon and/or hadronically Z boson, cross section for this process after all kinematic cuts could make a nearly two orders of magnitude difference between normal and inverted ordering of the neutrino mass hierarchy. We find that generic SM background events could be negligibly small after the application of kinematic cuts allowing for 5σ significance of these signals for different neutrino mass hierarchies in future. Finally we studied the left-right asymmetry from the same sign dilepton mode of mediating the doubly charged scalar boson. We find that positively charged di-muon final state could significantly deviate from the SM results and the corresponding deviations could be probed in the μ TRISTAN experiment with 3σ to 5σ significances in future.

ACKNOWLEDGMENTS

This work was supported by the Fundamental Research Funds for the Central Universities (TN, JL), the Natural Science Foundation of Sichuan Province under grant No. 2023NSFSC1329 and the National Natural Science Foundation of China under grant No. 11905149 (JL). The work of S.M. is supported by KIAS Individual Grants (PG086002) at Korea Institute for Advanced Study.

-
- [1] **Particle Data Group** Collaboration, P. A. Zyla *et al.*, “Review of Particle Physics,” *PTEP* **2020** no. 8, (2020) 083C01.
 - [2] S. Weinberg, “Baryon and Lepton Nonconserving Processes,” *Phys. Rev. Lett.* **43** (1979) 1566–1570.
 - [3] J. Schechter and J. W. F. Valle, “Neutrino Masses in $SU(2) \times U(1)$ Theories,” *Phys. Rev. D* **22** (1980) 2227.
 - [4] P. Minkowski, “ $\mu \rightarrow e\gamma$ at a Rate of One Out of 10^9 Muon Decays?,” *Phys. Lett. B* **67** (1977) 421–428.
 - [5] M. Gell-Mann, P. Ramond, and R. Slansky, “Complex Spinors and Unified Theories,” *Conf. Proc. C* **790927** (1979) 315–321, [arXiv:1306.4669 \[hep-th\]](#).
 - [6] T. Yanagida, “Horizontal gauge symmetry and masses of neutrinos,” *Conf. Proc. C* **7902131** (1979) 95–99.
 - [7] O. Sawada and A. Sugamoto, eds., *Proceedings: Workshop on the Unified Theories and the Baryon Number in the Universe: Tsukuba, Japan, February 13-14, 1979*. Natl.Lab.High Energy Phys., Tsukuba, Japan, 1979.
 - [8] R. N. Mohapatra and G. Senjanovic, “Neutrino Mass and Spontaneous Parity Nonconservation,” *Phys. Rev. Lett.* **44** (1980) 912.
 - [9] F. F. Deppisch, P. S. Bhupal Dev, and A. Pilaftsis, “Neutrinos and Collider Physics,” *New J. Phys.* **17** no. 7, (2015) 075019, [arXiv:1502.06541 \[hep-ph\]](#).
 - [10] A. Das, “Searching for the minimal Seesaw models at the LHC and beyond,” *Adv. High Energy Phys.* **2018** (2018) 9785318, [arXiv:1803.10940 \[hep-ph\]](#).
 - [11] P. D. Bolton, F. F. Deppisch, and P. S. Bhupal Dev, “Neutrinoless double beta decay versus other probes of heavy sterile neutrinos,” *JHEP* **03** (2020) 170, [arXiv:1912.03058 \[hep-ph\]](#).
 - [12] P. Coloma, E. Fernández-Martínez, M. González-López, J. Hernández-García, and Z. Pavlovic, “GeV-scale neutrinos: interactions with mesons and DUNE sensitivity,” *Eur. Phys. J. C* **81** no. 1, (2021) 78, [arXiv:2007.03701 \[hep-ph\]](#).
 - [13] P. B. Denton, “Sterile Neutrino Searches with MicroBooNE: Electron Neutrino Disappearance,” [arXiv:2111.05793 \[hep-ph\]](#).
 - [14] B. Dasgupta and J. Kopp, “Sterile Neutrinos,” *Phys. Rept.* **928** (2021) 63, [arXiv:2106.05913 \[hep-ph\]](#).
 - [15] P. Ballett, T. Boschi, and S. Pascoli, “Heavy Neutral Leptons from low-scale seesaws at the DUNE Near Detector,” *JHEP* **03** (2020) 111, [arXiv:1905.00284 \[hep-ph\]](#).
 - [16] S. Carbajal and A. M. Gago, “Indirect search of Heavy Neutral Leptons using the DUNE Near Detector,” [arXiv:2202.09217 \[hep-ph\]](#).
 - [17] J.-L. Tastet, E. Goudzovski, I. Timiryasov, and O. Ruchayskiy, “Projected NA62 sensitivity to heavy neutral lepton production in $K^+ \rightarrow \pi^0 e^+ N$ decays,” *Phys. Rev. D* **104** no. 5, (2021) 055005, [arXiv:2008.11654 \[hep-ph\]](#).
 - [18] A. Abada, D. Bečirević, O. Sumensari, C. Weiland, and R. Zukanovich Funchal, “Sterile neutrinos facing kaon physics experiments,” *Phys. Rev. D* **95** no. 7, (2017) 075023, [arXiv:1612.04737 \[hep-ph\]](#).
 - [19] **CMS** Collaboration, A. M. Sirunyan *et al.*, “Search for heavy neutral leptons in events with three charged leptons in proton-proton collisions at $\sqrt{s} = 13 \text{ TeV}$,” *Phys. Rev. Lett.* **120** no. 22, (2018) 221801, [arXiv:1802.02965 \[hep-ex\]](#).
 - [20] **CMS** Collaboration, A. M. Sirunyan *et al.*, “Search for heavy Majorana neutrinos in same-sign dilepton channels in proton-proton collisions at $\sqrt{s} = 13 \text{ TeV}$,” *JHEP* **01** (2019) 122, [arXiv:1806.10905 \[hep-ex\]](#).
 - [21] **CMS** Collaboration, A. Tumasyan *et al.*, “Probing Heavy Majorana Neutrinos and the Weinberg Operator through Vector Boson Fusion Processes in Proton-Proton Collisions at $s=13 \text{ TeV}$,” *Phys. Rev. Lett.* **131** no. 1, (2023) 011803,

- [arXiv:2206.08956](https://arxiv.org/abs/2206.08956) [hep-ex].
- [22] CMS Collaboration, A. Tumasyan *et al.*, “Search for long-lived heavy neutral leptons with displaced vertices in proton-proton collisions at $\sqrt{s} = 13$ TeV,” *JHEP* **07** (2022) 081, [arXiv:2201.05578](https://arxiv.org/abs/2201.05578) [hep-ex].
- [23] J. Schechter and J. W. F. Valle, “Neutrino Decay and Spontaneous Violation of Lepton Number,” *Phys. Rev. D* **25** (1982) 774.
- [24] M. Magg and C. Wetterich, “Neutrino Mass Problem and Gauge Hierarchy,” *Phys. Lett. B* **94** (1980) 61–64.
- [25] T. P. Cheng and L.-F. Li, “Neutrino Masses, Mixings and Oscillations in $SU(2) \times U(1)$ Models of Electroweak Interactions,” *Phys. Rev. D* **22** (1980) 2860.
- [26] G. Lazarides, Q. Shafi, and C. Wetterich, “Proton Lifetime and Fermion Masses in an $SO(10)$ Model,” *Nucl. Phys. B* **181** (1981) 287–300.
- [27] R. N. Mohapatra and G. Senjanovic, “Neutrino Masses and Mixings in Gauge Models with Spontaneous Parity Violation,” *Phys. Rev. D* **23** (1981) 165.
- [28] A. Das, P. Das, and N. Okada, “Testing neutrino mass hierarchy under type-II seesaw scenario in $U(1)_X$ from colliders,” [arXiv:2405.11820](https://arxiv.org/abs/2405.11820) [hep-ph].
- [29] S. Mandal, O. G. Miranda, G. Sanchez Garcia, J. W. F. Valle, and X.-J. Xu, “Toward deconstructing the simplest seesaw mechanism,” *Phys. Rev. D* **105** no. 9, (2022) 095020, [arXiv:2203.06362](https://arxiv.org/abs/2203.06362) [hep-ph].
- [30] S. Mandal, O. G. Miranda, G. S. Garcia, J. W. F. Valle, and X.-J. Xu, “High-energy colliders as a probe of neutrino properties,” *Phys. Lett. B* **829** (2022) 137110, [arXiv:2202.04502](https://arxiv.org/abs/2202.04502) [hep-ph].
- [31] P. F. de Salas, D. V. Forero, S. Gariazzo, P. Martínez-Miravé, O. Mena, C. A. Ternes, M. Tórtola, and J. W. F. Valle, “2020 global reassessment of the neutrino oscillation picture,” *JHEP* **02** (2021) 071, [arXiv:2006.11237](https://arxiv.org/abs/2006.11237) [hep-ph].
- [32] P. F. De Salas *et al.*, “Chi2 profiles from Valencia neutrino global fit,” 2021. <https://doi.org/10.5281/zenodo.4726908>.
- [33] DELPHI Collaboration, J. Abdallah *et al.*, “Search for doubly charged Higgs bosons at LEP-2,” *Phys. Lett. B* **552** (2003) 127–137, [arXiv:hep-ex/0303026](https://arxiv.org/abs/hep-ex/0303026).
- [34] ATLAS Collaboration, M. Aaboud *et al.*, “Search for doubly charged Higgs boson production in multi-lepton final states with the ATLAS detector using proton–proton collisions at $\sqrt{s} = 13$ TeV,” *Eur. Phys. J. C* **78** no. 3, (2018) 199, [arXiv:1710.09748](https://arxiv.org/abs/1710.09748) [hep-ex].
- [35] CMS Collaboration, “A search for doubly-charged Higgs boson production in three and four lepton final states at $\sqrt{s} = 13$ TeV,”.
- [36] ATLAS Collaboration, M. Aaboud *et al.*, “Search for doubly charged scalar bosons decaying into same-sign W boson pairs with the ATLAS detector,” *Eur. Phys. J. C* **79** no. 1, (2019) 58, [arXiv:1808.01899](https://arxiv.org/abs/1808.01899) [hep-ex].
- [37] CMS Collaboration, V. Khachatryan *et al.*, “Study of vector boson scattering and search for new physics in events with two same-sign leptons and two jets,” *Phys. Rev. Lett.* **114** no. 5, (2015) 051801, [arXiv:1410.6315](https://arxiv.org/abs/1410.6315) [hep-ex].
- [38] S. Antusch, O. Fischer, A. Hammad, and C. Scherb, “Low scale type II seesaw: Present constraints and prospects for displaced vertex searches,” *JHEP* **02** (2019) 157, [arXiv:1811.03476](https://arxiv.org/abs/1811.03476) [hep-ph].
- [39] J. De Blas, G. Durieux, C. Grojean, J. Gu, and A. Paul, “On the future of Higgs, electroweak and diboson measurements at lepton colliders,” *JHEP* **12** (2019) 117, [arXiv:1907.04311](https://arxiv.org/abs/1907.04311) [hep-ph].
- [40] ATLAS Collaboration, G. Aad *et al.*, “Search for doubly charged Higgs boson production in multi-lepton final states using 139 fb^{-1} of proton–proton collisions at $\sqrt{s} = 13$ TeV with the ATLAS detector,” *Eur. Phys. J. C* **83** no. 7, (2023) 605, [arXiv:2211.07505](https://arxiv.org/abs/2211.07505) [hep-ex].
- [41] ATLAS Collaboration, G. Aad *et al.*, “Search for doubly and singly charged Higgs bosons decaying into vector bosons in multi-lepton final states with the ATLAS detector using proton-proton collisions at $\sqrt{s} = 13$ TeV,” *JHEP* **06** (2021) 146, [arXiv:2101.11961](https://arxiv.org/abs/2101.11961) [hep-ex].
- [42] CMS Collaboration, V. Khachatryan *et al.*, “Search for a charged Higgs boson in pp collisions at $\sqrt{s} = 8$ TeV,” *JHEP* **11** (2015) 018, [arXiv:1508.07774](https://arxiv.org/abs/1508.07774) [hep-ex].
- [43] ATLAS Collaboration, M. Aaboud *et al.*, “Search for charged Higgs bosons decaying via $H^\pm \rightarrow \tau^\pm \nu_\tau$ in the τ +jets and τ +lepton final states with 36 fb^{-1} of pp collision data recorded at $\sqrt{s} = 13$ TeV with the ATLAS experiment,” *JHEP* **09** (2018) 139, [arXiv:1807.07915](https://arxiv.org/abs/1807.07915) [hep-ex].
- [44] ATLAS Collaboration, M. Aaboud *et al.*, “Search for charged Higgs bosons decaying into top and bottom quarks at $\sqrt{s} = 13$ TeV with the ATLAS detector,” *JHEP* **11** (2018) 085, [arXiv:1808.03599](https://arxiv.org/abs/1808.03599) [hep-ex].
- [45] ATLAS Collaboration, M. Aaboud *et al.*, “Search for additional heavy neutral Higgs and gauge bosons in the ditau final state produced in 36 fb^{-1} of pp collisions at $\sqrt{s} = 13$ TeV with the ATLAS detector,” *JHEP* **01** (2018) 055, [arXiv:1709.07242](https://arxiv.org/abs/1709.07242) [hep-ex].
- [46] CMS Collaboration, A. M. Sirunyan *et al.*, “Search for additional neutral MSSM Higgs bosons in the $\tau\tau$ final state in proton-proton collisions at $\sqrt{s} = 13$ TeV,” *JHEP* **09** (2018) 007, [arXiv:1803.06553](https://arxiv.org/abs/1803.06553) [hep-ex].
- [47] ATLAS Collaboration, M. Aaboud *et al.*, “Combination of searches for heavy resonances decaying into bosonic and leptonic final states using 36 fb^{-1} of proton-proton collision data at $\sqrt{s} = 13$ TeV with the ATLAS detector,” *Phys. Rev. D* **98** no. 5, (2018) 052008, [arXiv:1808.02380](https://arxiv.org/abs/1808.02380) [hep-ex].
- [48] C. A. Heusch and F. Cuypers, “Physics with like-sign muon beams in a TeV muon collider,” *AIP Conf. Proc.* **352** (1996) 219–231, [arXiv:hep-ph/9508230](https://arxiv.org/abs/hep-ph/9508230).
- [49] A. B. Arbuzov, S. G. Bondarenko, L. V. Kalinovskaya, L. A. Rumyantsev, and V. L. Yermolchik, “Electroweak effects in polarized muon-electron scattering,” *Phys. Rev. D* **105** no. 3, (2022) 033009, [arXiv:2112.09361](https://arxiv.org/abs/2112.09361) [hep-ph].
- [50] S. G. Bondarenko, L. V. Kalinovskaya, L. A. Rumyantsev, R. Sadykov, and V. L. Yermolchik, “One-Loop Electroweak Radiative Corrections to Polarized Møller Scattering,” *JETP Lett.* **115** no. 9, (2022) 495–501, [arXiv:2111.11490](https://arxiv.org/abs/2111.11490)

- [hep-ph].
- [51] Y. Hamada, R. Kitano, R. Matsudo, and H. Takaura, “Precision $\mu+\mu+$ and $\mu+e-$ elastic scatterings,” *PTEP* **2023** no. 1, (2023) 013B07, [arXiv:2210.11083 \[hep-ph\]](#).
- [52] Y. Hamada, R. Kitano, R. Matsudo, H. Takaura, and M. Yoshida, “ μ TRISTAN,” *PTEP* **2022** no. 5, (2022) 053B02, [arXiv:2201.06664 \[hep-ph\]](#).
- [53] K. Fridell, R. Kitano, and R. Takai, “Lepton flavor physics at $\mu^+\mu^+$ colliders,” *JHEP* **06** (2023) 086, [arXiv:2304.14020 \[hep-ph\]](#).
- [54] G. Lichtenstein, M. A. Schmidt, G. Valencia, and R. R. Volkas, “Complementarity of μ TRISTAN and Belle II in searches for charged-lepton flavour violation,” *Phys. Lett. B* **845** (2023) 138144, [arXiv:2307.11369 \[hep-ph\]](#).
- [55] P. S. B. Dev, J. Heeck, and A. Thapa, “Neutrino mass models at μ TRISTAN,” [arXiv:2309.06463 \[hep-ph\]](#).
- [56] M. Abe *et al.*, “A New Approach for Measuring the Muon Anomalous Magnetic Moment and Electric Dipole Moment,” *PTEP* **2019** no. 5, (2019) 053C02, [arXiv:1901.03047 \[physics.ins-det\]](#).
- [57] F. Bossi and P. Ciafaloni, “Lepton Flavor Violation at muon-electron colliders,” *JHEP* **10** (2020) 033, [arXiv:2003.03997 \[hep-ph\]](#).
- [58] M. Lu, A. M. Levin, C. Li, A. Agapitos, Q. Li, F. Meng, S. Qian, J. Xiao, and T. Yang, “The physics case for an electron-muon collider,” *Adv. High Energy Phys.* **2021** (2021) 6693618, [arXiv:2010.15144 \[hep-ph\]](#).
- [59] K. Cheung and Z. S. Wang, “Physics potential of a muon-proton collider,” *Phys. Rev. D* **103** (2021) 116009, [arXiv:2101.10476 \[hep-ph\]](#).
- [60] J.-C. Yang, Z.-B. Qing, X.-Y. Han, Y.-C. Guo, and T. Li, “Tri-photon at muon collider: a new process to probe the anomalous quartic gauge couplings,” *JHEP* **22** (2020) 053, [arXiv:2204.08195 \[hep-ph\]](#).
- [61] W. Liu and K.-P. Xie, “Probing electroweak phase transition with multi-TeV muon colliders and gravitational waves,” *JHEP* **04** (2021) 015, [arXiv:2101.10469 \[hep-ph\]](#).
- [62] J.-L. Yang, C.-H. Chang, and T.-F. Feng, “The leptonic di-flavor and di-number violation processes at high energy $\mu^\pm\mu^\pm$ colliders,” [arXiv:2302.13247 \[hep-ph\]](#).
- [63] A. Das, T. Nomura, and T. Shimomura, “Multi muon/anti-muon signals via productions of gauge and scalar bosons in a $U(1)_{L_\mu-L_\tau}$ model at muonic colliders,” *Eur. Phys. J. C* **83** no. 9, (2023) 786, [arXiv:2212.11674 \[hep-ph\]](#).
- [64] J. A. Casas and A. Ibarra, “Oscillating neutrinos and muon $\rightarrow e, \gamma$,” *Nucl. Phys.* **B618** (2001) 171–204, [arXiv:hep-ph/0103065 \[hep-ph\]](#).
- [65] S. Antusch, C. Biggio, E. Fernandez-Martinez, M. B. Gavela, and J. Lopez-Pavon, “Unitarity of the Leptonic Mixing Matrix,” *JHEP* **10** (2006) 084, [arXiv:hep-ph/0607020 \[hep-ph\]](#).
- [66] A. Abada, C. Biggio, F. Bonnet, M. B. Gavela, and T. Hambye, “Low energy effects of neutrino masses,” *JHEP* **12** (2007) 061, [arXiv:0707.4058 \[hep-ph\]](#).
- [67] S. Antusch and O. Fischer, “Non-unitarity of the leptonic mixing matrix: Present bounds and future sensitivities,” *JHEP* **10** (2014) 094, [arXiv:1407.6607 \[hep-ph\]](#).
- [68] M. Aoki, S. Kanemura, M. Kikuchi, and K. Yagyu, “Radiative corrections to the Higgs boson couplings in the triplet model,” *Phys. Rev. D* **87** no. 1, (2013) 015012, [arXiv:1211.6029 \[hep-ph\]](#).
- [69] J. Alwall, R. Frederix, S. Frixione, V. Hirschi, F. Maltoni, O. Mattelaer, H. S. Shao, T. Stelzer, P. Torrielli, and M. Zaro, “The automated computation of tree-level and next-to-leading order differential cross sections, and their matching to parton shower simulations,” *JHEP* **07** (2014) 079, [arXiv:1405.0301 \[hep-ph\]](#).
- [70] A. Alloul, N. D. Christensen, C. Degrande, C. Duhr, and B. Fuks, “FeynRules 2.0 - A complete toolbox for tree-level phenomenology,” *Comput. Phys. Commun.* **185** (2014) 2250–2300, [arXiv:1310.1921 \[hep-ph\]](#).
- [71] T. Sjostrand, S. Mrenna, and P. Z. Skands, “A Brief Introduction to PYTHIA 8.1,” *Comput. Phys. Commun.* **178** (2008) 852–867, [arXiv:0710.3820 \[hep-ph\]](#).
- [72] DELPHES 3 Collaboration, J. de Favereau, C. Delaere, P. Demin, A. Giammanco, V. Lemaître, A. Mertens, and M. Selvaggi, “DELPHES 3, A modular framework for fast simulation of a generic collider experiment,” *JHEP* **02** (2014) 057, [arXiv:1307.6346 \[hep-ex\]](#).
- [73] T. Chen and C. Guestrin, “Xgboost: A scalable tree boosting system,” in *Proceedings of the 22nd ACM SIGKDD International Conference on Knowledge Discovery and Data Mining*, KDD ’16. ACM, Aug., 2016. <http://dx.doi.org/10.1145/2939672.2939785>.
- [74] CMS Collaboration, A. Hayrapetyan *et al.*, “Search for heavy neutral leptons in final states with electrons, muons, and hadronically decaying tau leptons in proton-proton collisions at $\sqrt{s} = 13$ TeV,” *JHEP* **06** (2024) 123, [arXiv:2403.00100 \[hep-ex\]](#).
- [75] CMS Collaboration, A. Hayrapetyan *et al.*, “Review of searches for vector-like quarks, vector-like leptons, and heavy neutral leptons in proton-proton collisions at $\sqrt{s} = 13$ TeV at the CMS experiment,” [arXiv:2405.17605 \[hep-ex\]](#).
- [76] J. de Blas, “Electroweak limits on physics beyond the Standard Model,” *EPJ Web Conf.* **60** (2013) 19008, [arXiv:1307.6173 \[hep-ph\]](#).
- [77] F. del Aguila, J. de Blas, and M. Perez-Victoria, “Effects of new leptons in Electroweak Precision Data,” *Phys. Rev. D* **78** (2008) 013010, [arXiv:0803.4008 \[hep-ph\]](#).
- [78] E. Akhmedov, A. Kartavtsev, M. Lindner, L. Michaels, and J. Smirnov, “Improving Electro-Weak Fits with TeV-scale Sterile Neutrinos,” *JHEP* **05** (2013) 081, [arXiv:1302.1872 \[hep-ph\]](#).
- [79] ATLAS Collaboration, G. Aad *et al.*, “Search for heavy Majorana neutrinos with the ATLAS detector in pp collisions at $\sqrt{s} = 8$ TeV,” *JHEP* **07** (2015) 162, [arXiv:1506.06020 \[hep-ex\]](#).
- [80] CMS Collaboration, V. Khachatryan *et al.*, “Search for heavy Majorana neutrinos in $\mu^\pm\mu^\pm$ + jets events in proton-proton collisions at $\sqrt{s} = 8$ TeV,” *Phys. Lett. B* **748** (2015) 144–166, [arXiv:1501.05566 \[hep-ex\]](#).

- [81] **L3** Collaboration, P. Achard *et al.*, “Search for heavy isosinglet neutrino in e^+e^- annihilation at LEP,” *Phys. Lett. B* **517** (2001) 67–74, [arXiv:hep-ex/0107014](#).
- [82] **ATLAS** Collaboration, G. Aad *et al.*, “Search for heavy neutral leptons in decays of W bosons produced in 13 TeV pp collisions using prompt and displaced signatures with the ATLAS detector,” *JHEP* **10** (2019) 265, [arXiv:1905.09787 \[hep-ex\]](#).
- [83] **DELPHI** Collaboration, P. Abreu *et al.*, “Search for neutral heavy leptons produced in Z decays,” *Z. Phys. C* **74** (1997) 57–71. [Erratum: *Z.Phys.C* 75, 580 (1997)].
- [84] E. J. Chun, A. Das, S. Mandal, M. Mitra, and N. Sinha, “Sensitivity of Lepton Number Violating Meson Decays in Different Experiments,” *Phys. Rev. D* **100** no. 9, (2019) 095022, [arXiv:1908.09562 \[hep-ph\]](#).
- [85] **ATLAS** Collaboration, “Search for heavy neutral leptons in decays of W bosons using a dilepton displaced vertex in $\sqrt{s} = 13$ TeV pp collisions with the ATLAS detector,” [arXiv:2204.11988 \[hep-ex\]](#).
- [86] **ATLAS** Collaboration, G. Aad *et al.*, “Exploration at the high-energy frontier: ATLAS Run 2 searches investigating the exotic jungle beyond the Standard Model,” [arXiv:2403.09292 \[hep-ex\]](#).
- [87] **ATLAS** Collaboration, G. Aad *et al.*, “Search for heavy right-handed Majorana neutrinos in the decay of top quarks produced in proton–proton collisions at $\sqrt{s} = 13$ TeV with the ATLAS detector,” [arXiv:2408.05000 \[hep-ex\]](#).
- [88] **ATLAS** Collaboration, G. Aad *et al.*, “Search for Majorana neutrinos in same-sign WW scattering events from pp collisions at $\sqrt{s} = 13$ TeV,” *Eur. Phys. J. C* **83** no. 9, (2023) 824, [arXiv:2305.14931 \[hep-ex\]](#).
- [89] **ATLAS** Collaboration, G. Aad *et al.*, “Search for heavy Majorana neutrinos in $e^\pm e^\pm$ and $e^\pm \mu^\pm$ final states via WW scattering in pp collisions at $s=13$ TeV with the ATLAS detector,” *Phys. Lett. B* **856** (2024) 138865, [arXiv:2403.15016 \[hep-ex\]](#).
- [90] **FCC-ee study Team** Collaboration, A. Blondel, E. Graverini, N. Serra, and M. Shaposhnikov, “Search for Heavy Right Handed Neutrinos at the FCC-ee,” *Nucl. Part. Phys. Proc.* **273-275** (2016) 1883–1890, [arXiv:1411.5230 \[hep-ex\]](#).
- [91] S. Alekhin *et al.*, “A facility to Search for Hidden Particles at the CERN SPS: the SHiP physics case,” *Rept. Prog. Phys.* **79** no. 12, (2016) 124201, [arXiv:1504.04855 \[hep-ph\]](#).
- [92] **SHiP** Collaboration, C. Ahdida *et al.*, “Sensitivity of the SHiP experiment to Heavy Neutral Leptons,” *JHEP* **04** (2019) 077, [arXiv:1811.00930 \[hep-ph\]](#).
- [93] **NA62** Collaboration, E. Cortina Gil *et al.*, “The Beam and detector of the NA62 experiment at CERN,” *JINST* **12** no. 05, (2017) P05025, [arXiv:1703.08501 \[physics.ins-det\]](#).
- [94] **NA62** Collaboration, E. Cortina Gil *et al.*, “Search for heavy neutral lepton production in K^+ decays,” *Phys. Lett. B* **778** (2018) 137–145, [arXiv:1712.00297 \[hep-ex\]](#).
- [95] **NA62** Collaboration, G. Lanfranchi, “Search for Hidden Sector particles at NA62,” *PoS EPS-HEP2017* (2017) 301.
- [96] M. Drewes, J. Hajer, J. Klaric, and G. Lanfranchi, “NA62 sensitivity to heavy neutral leptons in the low scale seesaw model,” *JHEP* **07** (2018) 105, [arXiv:1801.04207 \[hep-ph\]](#).
- [97] D. Curtin *et al.*, “Long-Lived Particles at the Energy Frontier: The MATHUSLA Physics Case,” *Rept. Prog. Phys.* **82** no. 11, (2019) 116201, [arXiv:1806.07396 \[hep-ph\]](#).
- [98] F. Kling and S. Trojanowski, “Heavy Neutral Leptons at FASER,” *Phys. Rev. D* **97** no. 9, (2018) 095016, [arXiv:1801.08947 \[hep-ph\]](#).
- [99] **FASER** Collaboration, H. Abreu *et al.*, “The FASER Detector,” [arXiv:2207.11427 \[physics.ins-det\]](#).
- [100] **CHARM** Collaboration, F. Bergsma *et al.*, “A Search for Decays of Heavy Neutrinos in the Mass Range 0.5-GeV to 2.8-GeV,” *Phys. Lett. B* **166** (1986) 473–478.
- [101] **CHARM II** Collaboration, P. Vilain *et al.*, “Search for heavy isosinglet neutrinos,” *Phys. Lett. B* **343** (1995) 453–458.
- [102] J. Orloff, A. N. Rozanov, and C. Santoni, “Limits on the mixing of tau neutrino to heavy neutrinos,” *Phys. Lett. B* **550** (2002) 8–15, [arXiv:hep-ph/0208075](#).
- [103] S. A. Baranov *et al.*, “Search for heavy neutrinos at the IHEP-JINR neutrino detector,” *Phys. Lett. B* **302** (1993) 336–340.
- [104] G. Bernardi *et al.*, “FURTHER LIMITS ON HEAVY NEUTRINO COUPLINGS,” *Phys. Lett. B* **203** (1988) 332–334.
- [105] A. Boyarsky, O. Ruchayskiy, and M. Shaposhnikov, “The Role of sterile neutrinos in cosmology and astrophysics,” *Ann. Rev. Nucl. Part. Sci.* **59** (2009) 191–214, [arXiv:0901.0011 \[hep-ph\]](#).
- [106] O. Ruchayskiy and A. Ivashko, “Restrictions on the lifetime of sterile neutrinos from primordial nucleosynthesis,” *JCAP* **10** (2012) 014, [arXiv:1202.2841 \[hep-ph\]](#).
- [107] A. de Gouvea, W.-C. Huang, and J. Jenkins, “Pseudo-Dirac Neutrinos in the New Standard Model,” *Phys. Rev. D* **80** (2009) 073007, [arXiv:0906.1611 \[hep-ph\]](#).
- [108] A. de Gouvea, “See-saw energy scale and the LSND anomaly,” *Phys. Rev. D* **72** (2005) 033005, [arXiv:hep-ph/0501039](#).
- [109] M. Cirelli, G. Marandella, A. Strumia, and F. Vissani, “Probing oscillations into sterile neutrinos with cosmology, astrophysics and experiments,” *Nucl. Phys. B* **708** (2005) 215–267, [arXiv:hep-ph/0403158](#).
- [110] **MEG** Collaboration, J. Adam *et al.*, “New constraint on the existence of the $\mu^+ \rightarrow e^+ \gamma$ decay,” *Phys. Rev. Lett.* **110** (2013) 201801, [arXiv:1303.0754 \[hep-ex\]](#).
- [111] **BaBar** Collaboration, B. Aubert *et al.*, “Searches for Lepton Flavor Violation in the Decays $\tau_{+-} \rightarrow e_{+-} \gamma$ and $\tau_{+-} \rightarrow \mu_{+-} \gamma$,” *Phys. Rev. Lett.* **104** (2010) 021802, [arXiv:0908.2381 \[hep-ex\]](#).
- [112] **eBOSS** Collaboration, S. Alam *et al.*, “Completed SDSS-IV extended Baryon Oscillation Spectroscopic Survey: Cosmological implications from two decades of spectroscopic surveys at the Apache Point Observatory,” *Phys. Rev. D* **103** no. 8, (2021) 083533, [arXiv:2007.08991 \[astro-ph.CO\]](#).

- [113] T. Nomura, H. Okada, and H. Yokoya, “Discriminating leptonic Yukawa interactions with doubly charged scalar at the ILC,” *Nucl. Phys. B* **929** (2018) 193–206, [arXiv:1702.03396 \[hep-ph\]](#).